T.R.
BOLU ABANT İZZET BAYSAL UNIVERSITY
INSTITUTE OF GRADUATE STUDIES
DEPARTMENT OF CHEMISTRY

MOLECULAR DESIGN STUDY, SYNTHESIS, AND APPLICATIONS OF NOVEL MINOXIDIL DERIVATIVES

MASTER OF SCİENCE

NABAA NOUMAN HAMID HAMID

ACADEMIC SUPERVISOR
Prof. IZZET MORKAN
ACADEMIC CO-SUPERVIZOR
ASST. PROF. DR. MOHAMMED ODAY EZZAT

BOLU, APRIL 2024

APPROVAL OF THE THESIS

MOLECULAR DESIGN STUDY, SYNTHESIS, AND APPLICATIONS OF NOVEL MINOXIDIL DERIVATIVES submitted by **NABAA NOUMAN HAMID HAMID** and defended before the Examining Committe Members listed below in partial fulfillment of the requirements for the degree of **Master of Science** in **Department of Chemistry, Institute of Graduate Studies of Bolu Abant Izzet Baysal University in 18.04.2024** by

Examining Committee Members	**Signature**
Supervisor Prof. Dr. İzzet Morkan Bolu Abant izzet baysal university	.....
Member Prof. Dr. Mecit AKSU Düzce University	.....
Member Doç. Dr. Ercan Selçuk ÜNLÜ Bolu Abant İzzet Baysal Universit	.....

Prof. Dr. İbrahim KÜRTÜL

Director of Instıtute of Graduate Studies

ETHICAL DECLARATION

In this thesis dissertation that was properly prepared according to the Thesis Writing Rules of Bolu Abant İzzet Baysal University of the Institute of Graduates Studies, I hereby declare that;

- All data, information, and documents presented in the thesis were obtained in accordance with the academic and ethical rules,
- All data, documents, assessments, and results were presented in accordance with the scientific ethical and moral rules,
- All works that were benefitted in the thesis were appropriately cited,
- No alteration was made in the data used,
- Study presented in this thesis is original,

Otherwise, I declare that I accept the loss of all my rights in case any contradiction that may arise against me.

The similarity rate obtained by using the Turnitin program, a plagiarism detection software, is within the limits approved by the University Senate.

_____

NABAA HAMID

ABSTRACT

MOLECULAR DESIGN STUDY, SYNTHESIS, AND APPLICATIONS OF NOVEL MINOXIDIL DERIVATIVES
MSC THESIS
NABAA NOUMAN HAMID HAMID

BOLU ABANT IZZET BAYSAL UNIVERSITY
INSTITUTE OF GRADUATE STUDIES
DEPARTMENT OF CHEMISTRY
(SUPERVISOR: PROF. DR. IZZET MORKAN)
(CO-SUPERVISOR: ASST. PROF. DR. MOHAMMED ODAY EZZAT)
BOLU, APRIL 2024
(xii + 55)

In this study, 20 minoxidil derivatives are designed by using ChemDraw software, optimized with Chem3D. The energy is minimized by using Gaussian 09 with quantum mechanical treatment. The optimized structures are used as input (ligands) for Swissdock. Two cancers are selected to test the efficacy of compounds against it. In these cancers, we hypothesize that certain recognized proteins interact with the compounds causing inhibition of cancer. The proteins are 2R3J and 2IOG. binding affinity (ΔG) are calculated. The top four derivatives against every proteins are selected. In total, ΔG-Calculations indicated that compound C1 has the highest inhibitory activity against mammary gland breast cancer with (ΔG = − 6.138). C4 has the highest inhibitory activity against colorectal carcinoma with (ΔG = − 6.992). Measurements of HOMO, LUMO, and GAP indicate that molecules tend to behave more like acids than bases and have high kinetic activity but limited stability. All compounds obeyed Lipinski's rule according to ADMET prediction. The biological activity of compound C1 is (19.15 ± 1.01) against mammary gland breast cancer. C4 is (14.32±1.10) against colorectal carcinoma. These results demonstrate the potential of the synthesized compounds to act as anticancer drugs against these strains by inhibiting or deactivating the target proteins.

KEYWORDS: Computational chemistry, molecular docking. Theoretical studies, AMDET, anticancer, minoxidil, biological activity.

ÖZET

MOKÜLER TASARIM ÇALIŞMALARI, YENİ TÜR MONOOKSİDİL TÜREVLERİNİN SENTEZİ VE UYGULAMALARI
YÜKSEK LİSANS TEZİ
NABAA NOUMAN HAMID HAMID

BOLU ABANT İZZET BAYSAL ÜNİVERSİTESİ
LİSANSÜSTÜ EĞİTİM ENSTİTÜSÜ
KİMYA ANABİLİM DALI
(TEZ DANIŞMANI: PROF. DR. İZZET MORKAN)
(İKİNCİ DANIŞMAN: ASST. PROF. DR. MOHAMMED ODAY EZZAT)
BOLU, NİSAN - 2024
(xii + 55)

Bu çalışmada Chem3D ile optimize edilmiş ChemDraw yazılımı kullanılarak 20 adet minoksidil türevi tasarlanmıştır. Kuantum mekaniksel işlemlerde, Gaussian 09 kullanıarak yapıların enerjisi en aza indirilir. Optimize edilmiş yapılar Swissdock için girdi (ligandlar) olarak kullanılır. Bileşiklerin etkinliğini test etmek için iki kansed türü seçilir, bu kanserlerde, bilinen bazı proteinlerin, kanserin engellenmesine neden olan bileşiklerle etkileşime girdiğini varsayıyoruz. Proteinler 2R3J ve 2IOG'dır. Bağlanma afinitesi (ΔG) hesaplanır. Her proteine karşı ilk dört türev seçilir, ve toplamda, ΔG Hesaplamalarde, C1 bileşiğinin meme bezi kanserine karşı (ΔG =-6.138) en yüksek önleyici aktiviteye sahip olduğunu göstermiştir. C2, (ΔG = −6,992) ise kolorektal karsinoma karşı en yüksek inhibitör aktiviteye sahip olduğu görunmüştür. HOMO, LUMO ve GAP ölçümleri , moleküllerin bazlardan çok asitler gibi davranma eğiliminde olduklarını ve yüksek kinetik aktiviteye ancak sınırlı stabiliteye sahip olduklarını göstermektedir. ADMET tahminine göre tüm bileşikler Lipinski kuralına uymuştur. C1 bileşiğinin meme bezi meme kanserine karşı biyolojik aktivitesi (19.15 ± 1.01)'dir. C4 ise, kolorektal karsinoma karşı dır (14,32±1,10). Bu sonuçlar, sentezlenen bileşiklerin, hedef proteinleri inhibe ederek veya devre dışı bırakarak bu suşlara karşı antibakteriyel ilaçlar olarak etki gösterme potansiyelini göstermektedir.

ANAHTAR KELİMELER: Hesaplamalı kimya, molekül yerleştirme, teorik hesaplamalar, AMDET, antikanser, minoksidil, biolojik aktivite.

TABLE OF CONTENTS

LIST OF FIGURES

Page

LIST OF TABLES

Page

LIST OF ABBREVIATIONS AND SYMBOLS

MM : molecular mechanics

A : 2,6-Diamino-4-chloropyrimidine

ADMET :Absorption, distribution, metabolism, excretion, and toxicity prediction

API : Active Pharmaceutical Ingredient

CI : Configuration interaction

DFT : Density functional theory

FDA : Food and Drug Administration

HOMO : highest occupied molecular orbital

LUMO : lowest unoccupied molecular orbital

FMOs : frontier molecular orbitals

EA : electron affinity

μ : Electronegativity

ω : global electrophilicity index

η : Hardness

S : softness

H-BA : hydrogen bonds acceptors

H-BD : hydrogen bond donar

HF : Hartree-Fock

HIA : Human Intestinal Absorption

HOB : Human oral bioavailability

RB : rotatable bon

DMSO : dimethyl sulfoxide

I : ionization potential

m.p : Melting points

TF : Thomas–Fermi model

M. wt : molecular mass

MP : Møller–Plesset perturbation theory

NMR : Nuclear Magnetic Resonance

IR : Infrared Spectroscopy

ACKNOWLEDGEMENTS

Firstly, I would want to express my gratitude to God for blessing me with success in my education and areas of my life.

I would like to thank my supervisor, Prof. Dr. IZZET MORKAN, for his help,

and kindness throughout my studies.

My thanks and appreciation to my good role model to my co-advisor ASST. PROF. DR. MOHAMMED ODAY EZZAT, for his support, valuable information and instructions, and continuous encouragement for me.

Finally, and most importantly, I'm grateful to my family, especially my parents, husband, and brothers, for their love and support.

1. INTRODUCTION

1.1 Preface

One of the initial pharmaceutical substances employed in contemporary medical practice for the purpose of cancer therapy was mechlorethamine, an alkylating agent belonging to the class of nitrogen mustards. Its efficacy in treating lymphomas was discovered during the 1940s. In the year 1956, the antimetabolite methotrexate achieved the significant milestone of being the inaugural medicine to successfully treat a solid tumor. Subsequently, in the subsequent year, a novel category of tumor-combating chemicals called pyrimidine analogs**.** Since then, many anti-cancer drugs have been developed and used successfully.[1]

The existing body of research has shown a multitude of pyrimidine derivatives that show potential as effective anti-neoplastic medicines. By doing further analysis of the underlying data, it is possible to identify other new compounds that possess anti-proliferative and/or related biological properties across many domains. Significantly, the rational design and synthesis of novel bioactive compounds may be accomplished by in silico methodologies, structural modifications, and molecular fusion of the fundamental backbone of the bioactive chemical. Further investigation is necessary to assess the biological activity of modified pyrimidines in the therapy of many cancer types that have proven challenging to treat with current cancer treatments. The biological activity of these two heterocycles will assist in formulating, categorizing, and implementing fresh approaches to the discovery of anticancer medicines.[2]

1.2 Computational Chemistry

Within the discipline of chemistry, computational chemistry is an interdisciplinary area that uses sophisticated computational tools, data science, computer science, and mathematics to study and resolve problems pertaining to chemistry and the chemical world. The field of machine learning (ML) and artificial intelligence (AI) has become highly appealing due to the perceived ability of artificial neural networks (ANN) to address a wide range of tasksThe field of computational chemistry encompasses the advancement of methodologies and resources aimed at simulating molecules, solids, chemical processes, their configurations and alterations, and chemical environments. Molecular mechanics (MM) simulations, semiempirical methods, Hartree-Fock (HF), Density Functional Theory (DFT), and semiempirical methods are common methodologies for molecule and material modeling.[3] Furthermore, computational chemistry can be used to simulate complicated systems, such as biological membranes, and investigate their behavior under various situations.[4] Computational chemistry has rationalized molecular design by predicting the features of compounds that have not yet been produced. The findings of molecular computations allow a preliminary selection of potential compounds from a wider range of options; Just the most promising Molecules are then synthesized and actually examined.[5]

Quantum mechanics (QM or ab initio methods) and molecular mechanics (MM or empirical methods) are two computational techniques that are commonly used in the field of computational chemistry. The theoretical chemistry methods used in quantum mechanical (QM) computations include density functional theory (DFT) approaches, Hartree-Fock, and post-Hartree-Fock. Which are implemented in computer programs like the Gaussian series software. These calculations aim to offer precise characterizations or forecasts of the electronic characteristics, molecular structure, and reaction processes of systems that contain many atoms. Quantum mechanics (QM) is very suitable and necessary for the analysis of chemical processes that entail electron mobility within molecules, such as the breaking or formation of chemical bonds. While quantum mechanical (QM) calculations are known for their high processing cost, molecular mechanics (MM) computations are frequently employed to characterize biological systems and the construction of materials containing hundreds to millions of atoms.[6]

1.2.1 Classical Method

The classical method is a method that uses Newton mechanics to model a molecular system. This branch is divided into two parts: molecular mechanics, and molecular dynamics simulations.

1.2.1.1 Molecular Mechanics (MM)

In the 1970s, the force field technique was referred to as molecular mechanics (MM). This method relies on the idea that potential energy, which is defined by molecular geometry, which is defined by the spatial coordinates of the atoms, may be used to characterize a molecular set of atoms. Traditional physical mechanics serves as the foundation for computations of potential energy.[7]

Molecular mechanics (MM) is an empirical approach for calculating molecular attributes that go beyond molecular geometry, such as heat of formation, strain energy, dipole moment, and vibrational frequencies. It uses molecular force fields to see molecules ranging from tiny solvent molecules to massive polypeptides as force fields. There are now many MM force fields accessible for simulations of biological macromolecules.[8]

One common use of the Molecular Mechanics Poisson-Boltzmann Surface Area (MM-PBSA) and Generalized Born Surface Area (MM-GBSA) methodologies is the prediction of binding free energies in drug design and discovery. Their high computational efficiency makes them suitable for use in virtual screening procedures as well. Therefore, for MM-PBSA and MM-GBSA binding energy estimations to be significant for drug design/discovery goals, they must correlate well with experimental activities.[9]

1.2.1.2 Molecular Dynamics

Molecular dynamics (MD) exploits Newton's second equation for motion and interatomic potentials to monitor the time-dependent motions of every atom in the simulation domain.MD calculations may be used to infer the microscopic mechanics of mass and energy transmission because they provide an understanding of the complex motion of individual molecules inside a structure. Within an MD simulation, boundary constraints appropriate for the system's geometry or symmetry are applied to the numerical solution of the classical equations of motion regulating the microscopic temporal evolution of a many-body system. Thus, the

MD approach, which is founded on the fundamental concepts of classical mechanics, can provide an overview of the microscopic dynamical action of the individual molecules that comprise a particular system. Molecular dynamics is also used for investigating specific phonon features like the density of state, dispersal relationship, relaxing time, and emission over surfaces. [10][11]

Researchers can use MD simulations to investigate behaviors that may be hard to see experimentally, resulting in a better grasp of the basic processes and mechanisms that regulate tangible behavior. However, MD simulations have multiple drawbacks. They necessitate precise energy field parameters that are available, adequate computer resources, and acceptable modeling hypotheses.[12]

1.2.2 Quantum Chemistry Model

The electronic Schrödinger equation may be solved using the ab initio quantum chemistry method, which allows theoretical chemists to address a variety of structural and thermochemical issues. One of the fundamental techniques in ab initio quantum chemistry is the density functional theory (DFT) approach, which uses functionals between electron density and ground state energy to determine the many-electron function.[13]

Quantum chemistry aims to characterize a broad spectrum of molecules and material characteristics precisely and comprehensively. Quantum Chemistry's influence has grown in step with advancements in theory, mathematics, and computers, causing the size of systems that Quantum Chemistry can describe to increase orders of magnitude. Predicting chemical characteristics at the atomic scale using the first principal method is a theoretical and computational difficulty. ML approaches are becoming increasingly important in improving the capabilities of quantum chemical computations. In the last 10 years, a lot of focus has been on using machine learning (ML) to forecast quantum-mechanical energies and other properties. This approach offers significant computational savings since it generates predictions based on molecular structure without directly solving the Schrodinger equation. Although most machine learning (ML) applications in chemistry have linked atomistic structure to desired attributes, a lot of work is being done to create ML-enhanced quantum chemical techniques, including directly employing ML to improve Materials and molecules' electronic structures.[14]

1.2.2.1 Ab Initio Methods

The ab initio technique, which centers on density functional theory, can anticipate a crystal's total energy and thermodynamic properties. When ab initio calculations grow more precise, they may give information that might be utilized in place of experimental data, which could be insufficient, in the CALPHAD (Computer Coupling of Phase Diagrams and Thermochemistry) synthesis of Gibbs free energy.[15]

The basic characteristics of materials can be determined using ab initio approaches based on quantum mechanics rules. The fundamental idea is the solution of the many-body Schrödinger equation for systems containing tens to thousands of atoms and electrons. The many-body Schrödinger equation for the system is as follows, given the location of a set of atom nuclei R and their electrons r:

$H\Psi Rr = E\Psi Rr$

Ψ (R, r): the system's wave function.

H: Hamiltonian.

E: It’s the total energy of the system's

The wave function-based method is a theoretical framework that is well described. One of the most straightforward approaches in quantum chemistry is the Hartree-Fock technique. This method leverages the variational theorem to derive an approximation solution, yielding reasonably accurate results for a wide range of characteristics. The density functional theory (DFT) provides an alternative to the Hartree-Fock technique. It is based on the Hohenberg-Kohn theorem, which suggests the electronic energy of the base state may be predicted only by electron density. Although various attempts have been made to calculate the precise energy function, Density Functional Theory (DFT) calculations on actual models can be used to predict material properties consistently.[16]

In addition, there are other models of the Ab initio such as Møller–Plesset Perturbation Theory (MP), and Configuration Interaction (CI)[17] and Coupled Cluster (CC).[18]

1.2.2.2 Semi Empirical Methods

Semiempirical quantum-mechanical (SM) approaches offer extra molecular model approximation in addition to the MM computation, enabling a deeper comprehension of the electron distribution represented by molecular orbitals. Using SM approaches molecular orbitals are approximated with just valence electrons included, at varied degrees of approximation. The fundamental action at the core of SM-Methods is parameterization. This suggests that a collection of parameters for a specific collection of substances (database) is developed from experimental data. This simplifies quantum chemical computations greatly.[19] Semiempirical (SE) techniques have a long tradition throughout quantum chemistry and have lately gained more attention. The primary SE approaches are based on approximations to Hartree-Fock (HF) theory. In the past ten years, the density functional tight binding (DFTB) method has also become more well-liked. This method was created using the DFT framework and is based on a Taylor expansion of energy with regard to reference density. Both SE approaches employ the minimum basic set with varied approaches to electron integrals, resulting in increased computing efficiency. As a result, SE techniques may be utilized to study ten times larger systems or to undertake 1000 times longer sampling with the same computing resources. These gains can be increased further by combining SE techniques with new computing architectures and algorithms.[20]

1.2.2.3 Density Functional Theory (DFT)

DFT is employed in theoretical physics as well as chemistry. DFT is one of the most extensively used approaches in quantum computations since it is applicable to a wide range of systems at relatively high speed and low costIt can determine the overall energy of a multi-particle system, the electrical density of the orbitals, as well as the physical and optical characteristics of the material.[21]

DFT evolved from the Thomas-Fermi (TF) model, which was developed in the 1920s by Llewellyn Thomas and Enrico Fermi. However, this model was not feasible until the 1960s, and since then, the DFT has been in a state of continual evolution, providing conclusions that are compatible with experimental evidence.[22]

A common solution to the Schrödinger equation for a multi-atomic system is based on a wavefunction of 3N, where N is the number of molecules of the

multiple system. These systems' solution equations are frequently complicated and difficult to solve. This challenge is solved in DFT by substituting the wave function with the density function, which has just three variables. It serves as a foundation for computations, making mathematical and physical handling easier. DFT In a nutshell, it converts a multi-particle system's quantum problem into a single-particle system's problem.[23]

DFT's benefits do not mean that it is perfect; there are difficulties in using it to describe molecular interactions, especially when the forces are small, such as the Van der Waals forces, certain conductor computations, and transition electron states.[24]

1.2.3 Molecular Descriptor

Molecular descriptors are mathematical models of molecular attributes that are developed using computational techniques. Molecular descriptors' numerical values are used for determining the physical and chemical properties of molecules. LogP is one instance of a molecular descriptor.; it is a quantitative measure of a compound's lipophilicity. This descriptor is calculated by examining how the molecule splits between an aqueous phase and a lipophilic phase, which is usually composed of water and n-octanol. The utilization of molecular descriptors facilitates the conduct of similarity searches inside molecular libraries by enabling the identification of compounds with analogous physical or chemical attributes, as determined by the congruity of values exhibited by the descriptors. ADMET prediction models use molecular descriptors to build a link between structure and property. These descriptors assist in the prediction of the ADMET characteristics of compounds by leveraging their respective descriptor values.[25]

Molecular descriptors employed in ADMET models are classed as one-dimensional (1D), two-dimensional (2D), or three-dimensional (3D) based on the degree of molecular representation necessary to compute the descriptor. The most basic sort of molecular descriptor is the 1D descriptor, which represents data extracted from the molecule's molecular formula. This information includes the molecular weight, the number, and the kind of atoms in the molecule.

2D descriptors are more complex than 1D descriptors since they frequently offer molecular information regarding the molecule's size, structure, and electronic dispersion. Calculating 2D descriptors is mostly determined by the quantity of the

database, and calculating parts of a molecule in the absence of data may produce misleading results.

The 3D descriptors primarily define features linked to the molecule's 3D conformation, such as intramolecular hydrogen bonding. Polar and nonpolar surface areas (PSA and NPSA, respectively) are instances of descriptors produced from computations based on the molecules' 3D structure. Complex calculations, like quantum mechanics, may be used to produce 3D descriptors that characterize the valence electron distribution in molecules.[26]

1.2.4 Computational Chemistry Programs

Many chemical software packages have been created utilizing data from both classical and quantum chemical models. Each of them offers a unique collection of characteristics and differs in terms of accuracy, intricacy, and usability. The Gaussian program, for example, operates on the basis of ab initio, semiempirical, and molecular mechanics calculations.[27]

In the field of medicinal chemistry, software is used much from developing drug compounds to predicting their effectiveness. Some were used to investigate enzymatic processes in the context of the whole protein. This study used a collection of these programs to investigate the efficacy of proposed minoxidil derivatives against anti-cancer.

1.2.5 In-silico & ADMET Prediction Models

The word 'in silico' means computer-assisted testing as well as being related to the more common biology phrases 'in vivo' and 'in vitro'. ADMET consists of five criteria: Absorption, distribution, metabolism, excretion, and toxicity. This prediction is important in drug design at all stages, as well as in the creation of efficacious compounds with better ADMET properties. Several criteria, including Drug-Likeness Criteria, were measured in this study.[28]

1.3 Cancer as a Problem

The term "cancer" encompasses a broad range of conditions. The term "it" pertains to the medical condition that arises as a result of biological modifications leading to uncontrolled proliferation and division of cells. Certain types of cancer facilitate rapid cellular proliferation, whilst others induce a more sluggish pace of cellular growth and division. Various forms of cancer are characterized by the presence of discernible neoplastic masses known as tumors, but certain kinds, such as leukemia, lack this particular manifestation. Cancerous cells may develop in one

location and subsequently spread across the lymph nodes.[29] Cancers can be classified in two ways: by the kind of tissue in which they develop (histological type) and by the primary site, or the region in the body where the cancer originally appeared.[30]

Cancer is the world's second greatest cause of death, accounting for one in every six deaths, according to the WHO. Researchers have put a lot of effort into diagnosing and treating tumors throughout the years. There is strong evidence linking the emergence of several cancers to environmental (acquired) variables, including pollution and radiation. A person's lifestyle, which may include food, use of tobacco products, smoking, stress, and inactivity, is a major factor in their chance of developing cancer. The contribution of DNA repair genes, proto-oncogene mutations, and tumor suppressor gene expression patterns to the genesis of cancer is difficult to measure, despite the fact that these environmental variables are now understood to have a significant role in the creation of cancer. Only 5–10% of cancer cases are caused by inheritance, and aging is another significant risk factor in addition to many others.[31] More than 100 forms of cancer have already been identified. Lungs, breast, prostate, colon, rectum, bronchus, bladder, skin, pelvic, kidney, leukemia, stomach, pancreas, cervical, and other cancers are the most prevalent. Breast cancer is the most common cancer among women. to be diagnosed, whereas in men, prostate cancer is the most common condition. Age-related increases in gallbladder cancer are more common in women.[32] In the world, cancer is now the second greatest cause of mortality after cardiovascular disease and a serious health issue.[33]

1.4 Minoxidil

Minoxidil (molecular formula $C_9H_{15}N_5O$) is a heterocyclic aromatic compound also known as: 6-Piperidin-1-ylpyrimidine-2,4-diamine 3-oxide, which is a pyrimidine derivative.[34] Figure (1-1)

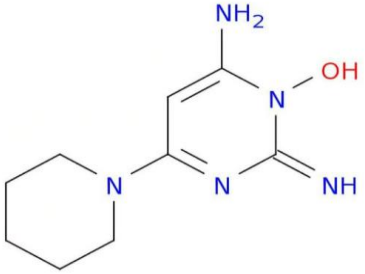

Figure 1-1 minoxidil structure.

Minoxidil, a prodrug, has been utilized as a type of oral hypertension since the 1960s. While it was first released to be a medication to control hypertension, it quickly gained popularity owing to its fortunate finding of increasing hair growth while stimulating new hair formation. This has resulted in the use of minoxidil in both topical and oral formulations to treat a variety of hair loss conditionsIn 1988, the FDA authorized topical minoxidil (TM) 2% for the treatment of male androgenetic alopecia (AGA) and female pattern hair loss (FPHL).[35]

Minoxidil is a peripheral vasodilator that reduces both systolic and diastolic blood pressure. which works by directly relaxing the smooth muscle of the arteries. Calcium channel activation is linked to its activity. Vascular tonicity requires calcium ion flow into smooth muscle cells, which is lowered when these channels are open, causing the cells to hyperpolarize. But when minoxidil is used, hypotension is accompanied by tachycardia, elevated renin secretion, and sodium and water ion retention. Owing to the potential for significant side effects, it is only used in concert with two other antihypertensive medicines and for severe hypertension that has not responded to prior drug treatment.[36]

1.5 Literature Reviews

Metwally et al. (2019) synthesized a novel sequence of pyrimidines and established their chemical composition using elemental and spectrum analysis. The MTT-Assay was used to examine the Cytotoxicity of a selection of compounds from the series on the breast MCF-7 and Hela malignant cell lines. Compounds Figure (1-2) exhibited higher cytotoxicity than the two cancer-cell-lines, with Doxorubicin acting as the control-medicine. Compounds 1, 2, and 3 showed significant efficacy in exerting inhibitory effects on histone lysine demethylases (KDM). Compound 2, which exhibited the highest level of KDM inhibition, was shown to induce cell cycle arrest at the G2/M stage, fourfold compared to the control. Additionally, it demonstrated a tenfold increase in overall apoptotic activity compared to the control. Lipinski's rule of five was applied during in-silico-Experiments using cytotoxically active compounds 1, 2, and 3. Furthermore, a molecular docking study was used to explain the manner in which actively hazardous compounds attach to enzymes. Additionally, an in-silico study was performed on analogs 2 and 3 using Swiss ADMET.[37]

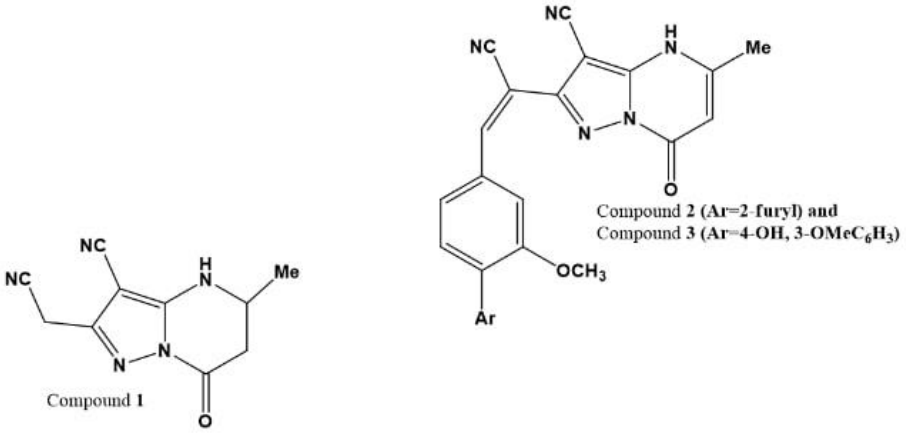

Figure 1-2 Active pyrazolo[1,5-a] pyrimidines analogues displaying cytotoxicity action via cell cycle detention at G2/M stage.

The potential of human kinesin Eg5 as an inhibitory target in cancer treatment has been acknowledged. Muthuraja et al. (2019) found that pyrazolopyrimidine compounds were potent Eg5 inhibitors, inhibiting the proliferation of mitotic kinesin. Exogenous inhibitors bind to Eg5 and cause metaphase obstruction, which leads to cell apoptosis. The IC50 values were calculated by comparing them to the Eg5 motor domain using ATPase steady-state analysis. To gain a better understanding, a molecular docking simulation was performed. The docking simulation results show that the inhibitors target two allosteric sites: helices α4 and α6, as well as helices α2, α3, and loopL5. Among the fifteen compounds examined, three pyrazolopyrimidine compounds (1, 2, and 3) Figrue (1-3) showed considerable inhibition of Eg5. The anti-proliferative effect of three analogues was tested in vitro against the HeLa cell line originating from cervical cancer. [38]

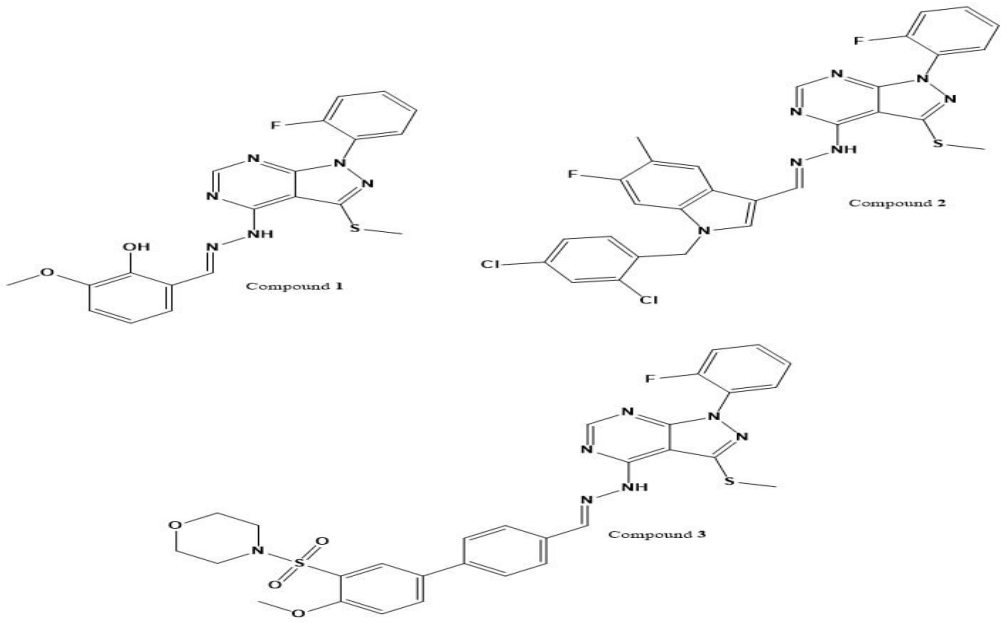

Figure 1-3 Active pyrazolopyrimidine derivatives (Compounds 1-3) which inhibit cell cycle at metaphase.

Eissa et al. (2020) developed a new class of pyrimidine-5-carbonitrile compounds that work as ATP-competitive tyrosine kinase inhibitors for the epidermal growth factor receptor (EGFR). The compounds were developed and evaluated for their in vitro cytotoxicity against four human malignant cell lines: HCT-116 (colorectal carcinoma), HepG-2 (hepatocellular carcinoma), MCF-7 (breast cancer), and A549 (non-small cell lung cancer cells). Figure (1-4) depict five compounds of the target chemical that were shown to have a mean anti-proliferative impact on the cell lines being investigation. According to the results of the cell cycle and apoptosis studies, compound 1 has the ability to arrest the cell cycle at the G2/M stage and produce considerable death in HepG-2, HCT-116, and MCF-7 cells. Furthermore, compound 1 exhibited a 6.5-fold increase in caspase-3 levels in the HepG-2 cell line when compared to the control grou.[39]

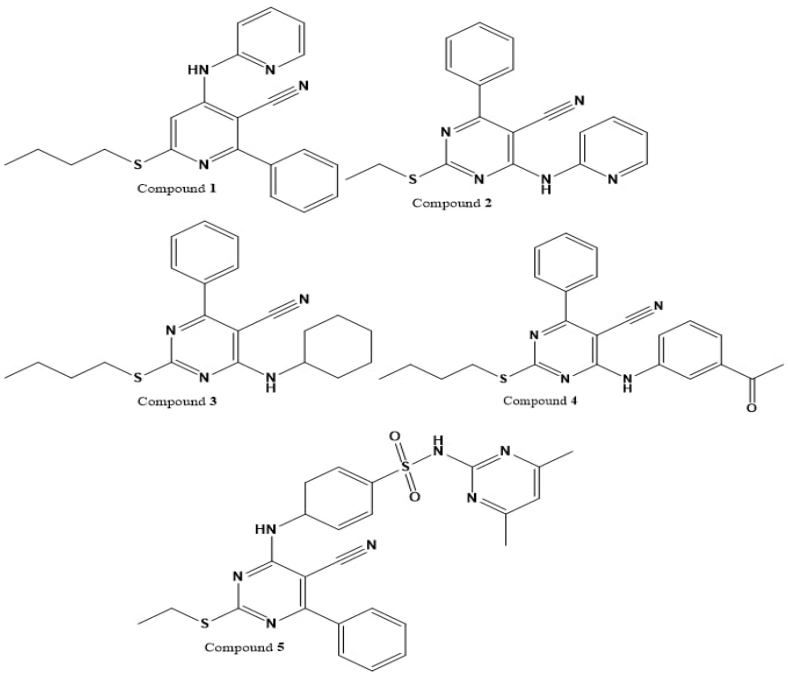

Figure 1-4 Active pyrimidine-5-carbonitrile analogues (Compounds 1-5) which seize the cell cycle at G2/M stage and stimulate apoptosis.

In their study, Wang et al. (2020) undertook the design and synthesis of a series of 2,7-disubstituted-thieno[3,2-d] pyrimidine derivatives with the aim of investigating their potential as novel inhibitors of focal adhesion kinase (FAK). A new kinase inhibitor stage, characterized by the presence of the fresh 2,7-disubstituted-thieno[3,2-d] pyrimidine skeleton, has been developed. This structure closely resembles the bioactive molecular arrangement of the well-known diaminopyrimidine motif. Most of the substances effectively obscured the enzymatic activities of FAK, resulting in a significant reduction in the growth of the cancer cell lines A-549, U-87MG, and MDA-MB-231. Compound 1, as shown in Figure 1–5, was the most effective in inhibiting the enzyme and had more potential in A–549, U–87MG, and MDA–MB-231 cells than TAE-226. Compound 1 exhibited a relatively lower degree of cytotoxicity towards HK2, a normal human cell line. In accordance with the results obtained from flow cytometry analysis, it was shown that compound 1 exhibited a dose-dependent induction of apoptosis in MDA-MB-231 cells. Additionally, compound 1 effectively arrested the progression of MDA-MB-231 cells at the G0/G1 phase of the cell cycle. Subsequent investigations have provided evidence indicating that compound 1 effectively inhibits the migration of MDA-MB-231 cells. In aggregate, the aforementioned facts support the further advancement of compound 1 as a leading candidate for the investigation of FAK-targeted anticancer drugs.[40]

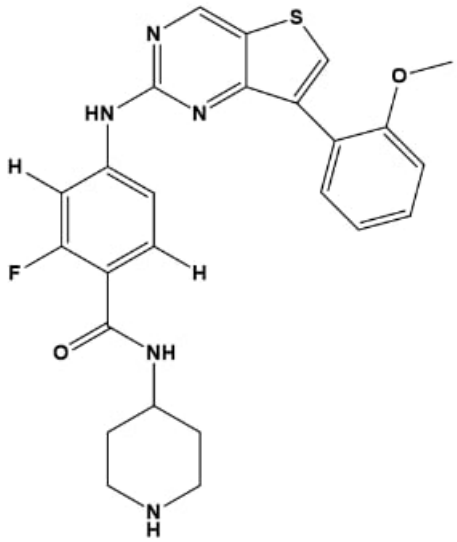

Figure 1-5 Active 2,7-disubstituted-thieno[3,2-d] pyrimidine derivative (compound 1) as active suppressor of MDA-MB-231 cells migration.

Bommera et al. (2021) observed notable anti-cancer efficacy in 1,2,4-oxadiazole derivatives during studying these chemicals against human malignant cell lines. Furthermore, these compounds demonstrated α and β 3-receptor antagonist, anti-helminthic, histamine-H3, antibacterial, antiparasitic, analgesic, anti-inflammatory, and antidiabetic effects. Figure (1-6) depicts a sequence of 10 compounds synthesized from 1,2,4-oxadiazole-linked 5-fluorouracil derivatives. Following that, the analogues were tested for anti-proliferative properties on four human cancer cell lines, MCF-7, MDA MB-231, A549, and DU-145, using the MTT assay. Analogues 1-4 and 9 outperformed the reference chemical in terms of anticancer activity.[41]

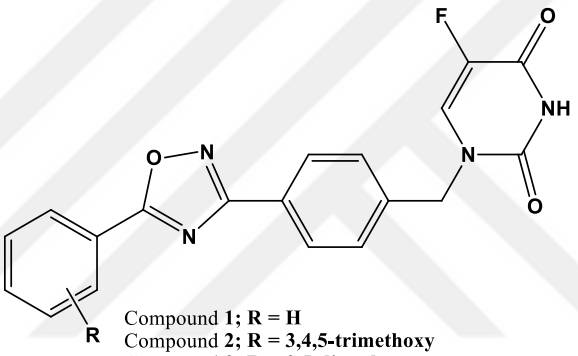

Compound **1; R = H**
Compound **2; R = 3,4,5-trimethoxy**
Compound **3; R = 3,5-dimethoxy**
Compound **4; R = 4-methoxy**
Compound **5; R = 4-chloro**
Compound **6; R = 4-bromo**
Compound **7; R = 4-nitro**
Compound **8; R = 3,5-dinitro**
Compound **9; R = 4-methyl**
Compound **10; R = 4-bromo-3,5-dinitro**

Figure 1-6 Active 1,2,4-oxadiazole derivatives (Compounds 1-10) displaying antiproliferative action.

2. AIM AND SCOPE OF THE STUDY

In this research:

1- Design and molecular optimization of Minoxidil derivatives series by molecular design software to identify the best scaffold.
2- Using molecular docking study to find the top 20 active compounds.
3- Appling DFT Analysis to determine HOMO, LUMO, GAP, ionization potential, electron affinity, electronegativity, hardness, softness, global electrophilicity index, and global electrophilicity index
4- Employing in-silico drug-likeness and ADMET prediction to study the possibility of using compounds as drugs.
5- Synthesis and characterization several effective compounds suggested and obtained from theoretical study.
6- Study and evaluation of the biological activities of the synthesized compounds.

3. MATERIALS AND METHODS

3.1 Materials Used

All the chemicals used in this study were of the highest purity possible, and they were used directly by the manufacturers with no additional processing.

No.	Substances	Molecular Formula	Company	Purity%
1	2,6-Diamino-4-Chloropyrimidine	$C_4H_5ClN_4$	Sigma-Aldrich®	98%
2	5-Amino-2-bromobenzoic acid	$C_7H_6BrNO_2$	Sigma-Aldrich®	94%
3	5-Aminosalicylic Acid	$H_2NC_6H_3$-2-(OH) CO_2H	Sigma-Aldrich®	99%
4	5-Amino-2-methylbenzoic acid	$H_2NC_6H_3(CH_3)$ CO_2H	Sigma-Aldrich®	99%
5	5-Amin-2 Chlorobenzoic Acid	$H_2NC_6H_3(Cl)CO_2H$	Sigma-Aldrich®	96%
6	Ethanol	CH_3CH_2OH	Scharlab	99%
7	Methanol	CH_3OH	Scharlab	99%
8	Benzene	C_6H_6	Scharlab	99%
9	N-Hexane	$CH_3(CH_2)_4CH_3$	Scharlab	99%
10	Dimethyl sulfoxide	$(CH_3)_2SO$	Scharlab	99%
11	Dimethylformamide	$HCON(CH_3)_2$	Scharlab	99%
12	Water	H_20		99%

Table 3-1 Chemicals are used.

3.2 Instruments and Software

No.	Tools and Equipment	Company	Origin
1	Chem Draw 20.0	PerkinElmer	Llantrisant United Kingdom
2	Chem3D 20.0	PerkinElmer	Llantrisant United Kingdom
3	Swissdock	Swiss Institute of Bioinformatics	Switzerland
4	Gaussian 09	Carnegie Mellon University	Pennsylvania, United States
5	AdmetSAR	Chinese Academy of Sciences	China
6	Nuclear magnetic resonance instrument (NMR)	Bruker Avance Neo 500 MHz	Germany
7	FT-IR spectrophotometer	Bruker	Germany
9	Liquid chromatography-mass spectrometry (LC-MS)	Bruker BioSpin GmbH	Germany

Table 3-2 Software and Equipment that are used.

3.3 Theoretical part: Computational Study

3.3.1 Chem Draw

The Chem Office (Chem Draw 20.0) with appropriate 2D orientation is used to design 683 suggested minoxidil, of which 20 are eventually selected for theoretical study. Arrange their sequence according to the best binding affinity for each protein separately.

3.3.2 Chem3D

The four derivatives (C1, C2, C3, C4) drawn into the chemigraphy, are treated using MM2 energy reduction for each compound using Chem3D 20.0.

3.3.3 DFT Analysis

The electronic structure, particularly the ground state, of the molecules under study is investigated and optimized using DFT analysis in Gaussian 09 (G9M216772357589W/3084N). The visualization of the results is performed using Gaussview6.0(<HID>5024786827262827292367182487543769758237762239764244763243426366</HID>). The basis set B3LYP/6-31G++ (d, p) is employed for this analysis. The investigation focuses on the relationship between the electronic structure and the geometry of the molecules, including optimal geometries, molecular electrostatic potential (MEP), Mulliken's atomic charges,

highest occupied molecular orbital (HOMO), lowest unoccupied molecular orbital (LUMO), and energy gap. Ultimately, these calculations aid in determining important variables such as reactive parameters, including electronegativity, the global electrophilicity index (ω), ionization potential, hardness (η), softness (S), redox potential, and electrophilicity.[42]

3.3.4 Molecular Docking

Swissdock of the Swiss Institute of Bioinformatics – Docking with standard procedure is used to dock the proteins (PDB ID: 2R3J and 2IOG) and suggested chemical compounds (C1, C2, C3, C4) into the active site of proteins. The DFT-optimized structures are used as input for Swissdock. From the Protein Data Bank, the crystal structures of receptor HCT-116 (colorectal carcinoma) and MCF-7 (mammary gland breast cancer) were obtained. Computational calculations were performed using Schro dinger Small Molecule Drug Discovery Suite (Schrodinger Release, 2018). The atomic coordinates for the protein were extracted from the X-ray crystal structures (PDB ID: 2R3J and 2IOG). The initial setup of the enzyme for calculations was prepared using the Protein Preparation Wizard of Schrodinger. The center of the grid box was situated using the location of co-crystallized original ligands and was refined and set up at 20 A°. To generate the minimized energy 3D structures, the LigPrep module was used under the OPLS-AA force field. Molecular docking studies were performed using Glide. Glide finds the best possible ligand binding position in a protein grid space, evaluating the energy interactions between them. In this study, the Maestro tool was used to perform rigid, flexible docking for predicting the binding affinity, ligand efficiency, and inhibitory constant of the target. The ligands were docked to the active site of the enzyme using Glide Extra Precision (XP), which dock to determine the ligand's flexibility. Only the active small molecule would have available access to avoid the penalties and receive favorable docking scores with accurate hydrophobic contact between the protein and ligand. The electrostatic energy interaction of the hydrogen-bonds involved both the side and back chains, hydrophobic contact, and salt bridge contacts.

3.3.5 In-Silico & ADMET Predictions

The proposed compounds' structure is converted into a Simplified Molecular-Input Line-Entry system (SMILE) using the admetsar 2.0 website (https://lmmd.ecust.edu.cn/admetsar2/result/?tid=549055). Following that, the chemical compounds were further subjected to in silico prediction of

pharmacokinetics by the same source. This involved assessing several parameters such as AlogP, H-Bond Acceptor, H-Bond Donor, Rotatable Bonds, Molecular Weight, and Applicability Domain. The technique was also utilized to predict the Human Intestinal Absorption and Human oral bioavailability.

3.4 Experimental Procedure

3.4.1 Synthesis of minoxidil derivatives (general procedure)

0.500 g of 2,6-Diamino-4-chloropyrimidine (A) are weighed with a sensitive balance, then placed in a 250 ml Round bottom flask with 100 ml of water. To synthesize C1, 0.528 g of 5-aminosalicylic acid is added to A. The solution is then regulated in reflux at 100ºC while stirring on a heating plate for 6 hours. To synthesise C2, 0.520 g of 5-Amino-2-methylbenzoic acid is added to solution A. 0.591 g of 5-Amino-2-chlorobenzoic acid are added to synthesize C3, and 0.745 gm of 5-Amino-2-bromobenzoic acid are used to synthesize C4 with the same steps for synthesize C1 as in the following reactions.

When the reaction is finished, the solution is left to cool at room temperature, then filtered and dried. The resulting precipitate is then washed in hot ethanol to crystallize the product for greater purity.[43]

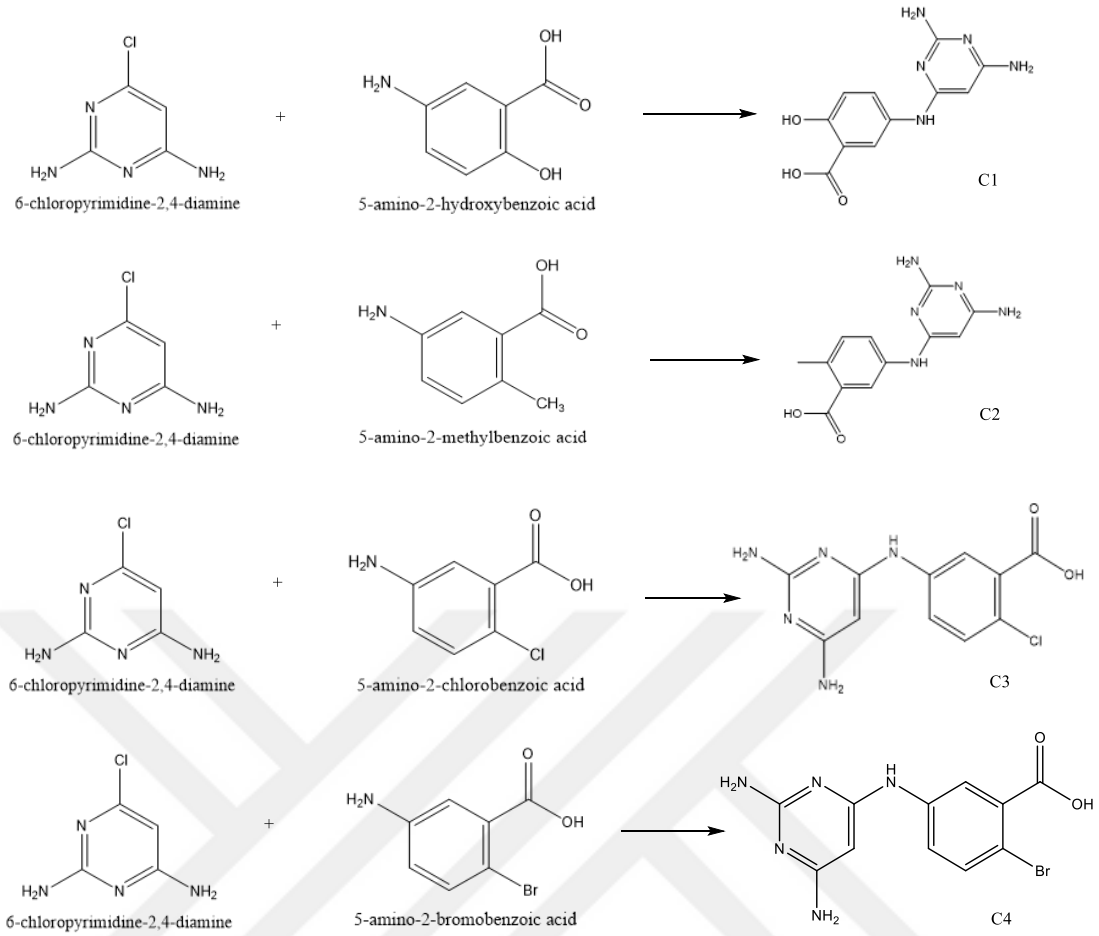

3.4.2 Solubility in Various Solvents

0.1 g from each synthetic compound were used and the solubility of these compounde were thested using 5 ml of ;distilled water, DMSO, DMF, hexane, methanol, and ethanol separately. The only solvent was DMSO at which the compounds were dissolved compeletly.

3.5 Spectroscopic Methods

3.5.1 FT-IR measurement

An infrared spectrometer (Bruker) was used to measure each of the about 2 mg of powdered samples (C1, C2, C3, and C4) that were obtained. The IR was read of the samples, which were recorded within the range of 400 cm^{-1} to 4000 cm^{-1} in the Department of Chemistry's research lab at Al-Mustansiriya University, College of Science.

3.5.2 NMR Measurements

^{1}H, ^{13}C NMR spectra for the prepared compounds were in DMSO using a Bruker Avance Neo 500 MHz at the research laboratory of the College of Pharmacy, Ankara University.

3.5.3 LCMS Measurements

The prepared compounds C1, C2, C3, and C4 were measured by mass spectrometry in type LC-mass (electrospray ionization is carried out by ESI (+) or (-) method) at the research laboratory of the College of Pharmacy, Ankara University.

3.6 Biological Activity

Two human cancer cell lines, specifically mammary adenocarcinoma (MCF-7) and colorectal cancer (HCT-116), were obtained from the USA. Reagents used in this study were RPMI-1640 medium, MTT, DMSO, and fetal bovine serum (GIBCO, United Kingdom). Doxorubicin was used as the reference anticancer agent for comparison purpose. The MTT assay was used to investigate the inhibitory effects of targeted drugs on cell proliferation in the above cell lines. Cells were cultured in RPMI-1640 medium supplemented with 10% fetal bovine serum. Then antibiotics were added: (100 µg/ml) penicillin and (100 units/ml) streptomycin, in a 5% CO_2 incubator at 37°C. Cells were then seeded for 48 h in a 96-well plate at a density of 1.0 × 104 cells/well at 37°C under 5% CO. After Incubation, cells were treated with different concentrations of compounds and incubated for 24 h. 20 µl of MTT solution at 5 mg/ml was added 24 h after drug treatment and incubated for 4 h. To dissolve the purple formazan formed, 100 µL of DMSO was added to each well. The colorimetric assay was measured and recorded at the absorbance of 570 nm using a plate reader (EXL 800, USA). Relative Cell Viability was calculated as a percentage.

4. RESULTS & DISCUSSIONS

4.1 Molecular Docking Studies

The approach of molecular docking is employed to forecast the optimal orientation, affinity, and interaction of a ligand inside the binding site of the protein. The utilization of preferred orientation data may be employed to make predictions regarding the binding affinity strength between a therapeutic target and a ligand molecule by employing scoring functions.[44] The determination of the degree of favorability of a reaction is provided by the concept of Gibbs Free Energy (ΔG). A larger negative value of ΔG signifies a stronger propensity for binding between a ligand and its target. However, in order to assess the degree of favorability of ΔG, it usually compared with a known standard. In this work, ΔG values were compared with Doxorubicin. Doxorubicin is an anticancer agent drug. In this study, Among 4 studied compounds; the 4-top minoxidil derivatives as anticancer activity towards two types of cancer: Compound C1 showed the highest binding affinity towards mammary gland breast cancer (MCF-7), and Compound C4 towards colorectal carcinoma (HCT-116).

By evaluating the interactions with the protein (2R3J), the binding affinity of the synthesized compounds to the protein ranged between (-8.154 _-6.992). The interactions between the compound and the protein. Compound C1 formed three hydrogen-bonds through (GIU8, LEU83, and GLU81), C2 and C3 formed two hydrogen-bonds through LEU83 and ASP145. C3 formed halogen bonding through CIU81. While C4, which has the highest binding affinity, formed hydrogen bonds through ILE10 and Asp145.

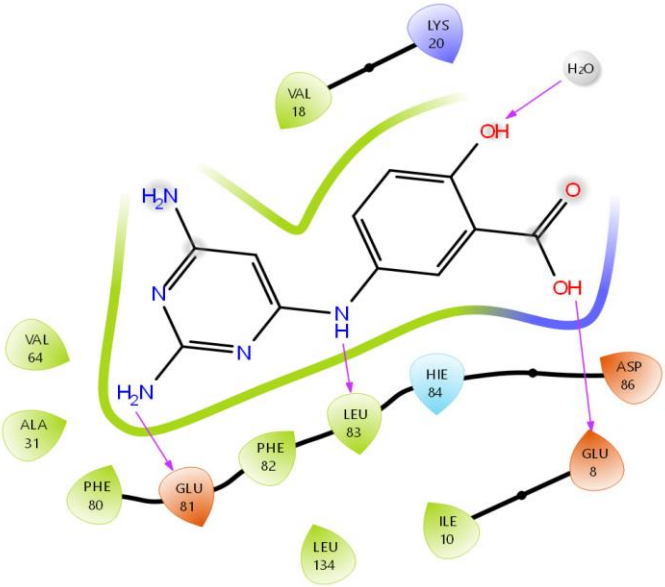
LYS 20
VAL 18
H2O
OH
O
H2N
N
N
H
N
H2N
VAL 64
ALA 31
PHE 80
GLU 81
PHE 82
LEU 83
HIE 84
ASP 86
GLU 8
ILE 10
LEU 134

C1

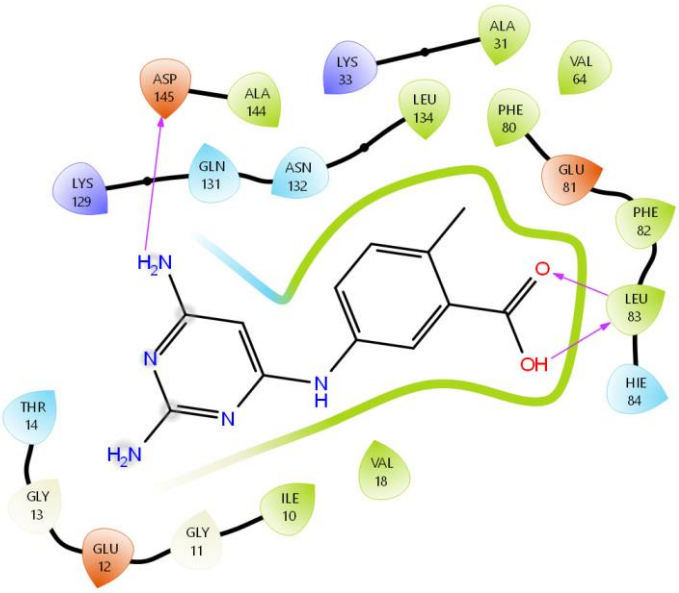
ALA 31
LYS 33
VAL 64
ASP 145
ALA 144
LEU 134
PHE 80
LYS 129
GLN 131
ASN 132
GLU 81
PHE 82
H2N
O
LEU 83
N
N
H
OH
HIE 84
N
H2N
THR 14
VAL 18
GLY 13
ILE 10
GLU 12
GLY 11

C2

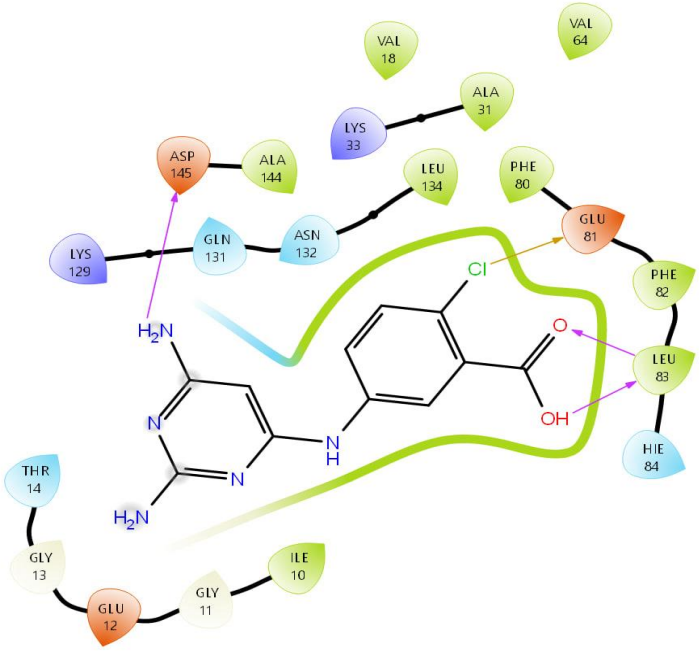
VAL 18
VAL 64
ALA 31
LYS 33
ASP 145
ALA 144
LEU 134
PHE 80
GLU 81
LYS 129
GLN 131
ASN 132
Cl
PHE 82
H2N
O
LEU 83
N
N
H
OH
HIE 84
N
H2N
THR 14
GLY 13
ILE 10
GLU 12
GLY 11

C3

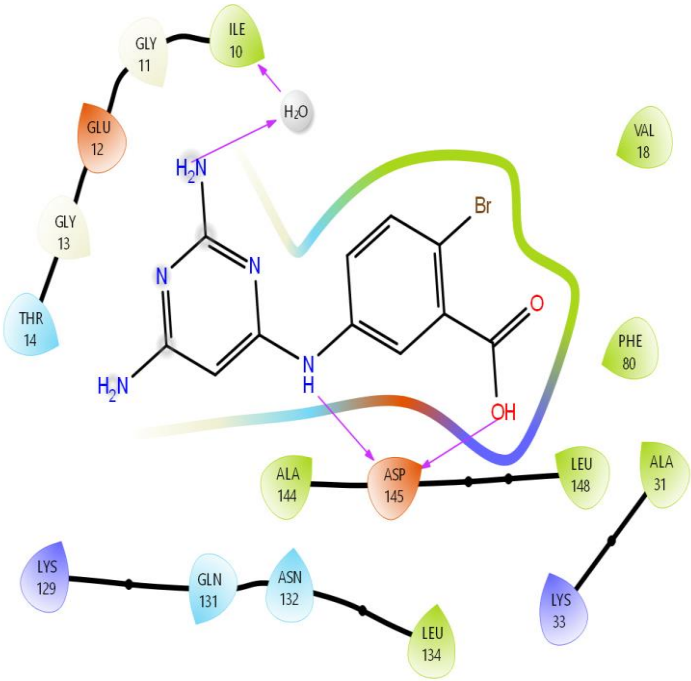
GLY 11
ILE 10
GLU 12
H2O
VAL 18
H2N
Br
GLY 13
N
N
O
THR 14
PHE 80
N
H
OH
H2N
ALA 144
ASP 145
LEU 148
ALA 31
LYS 129
GLN 131
ASN 132
LYS 33
LEU 134

C4

As for the binding affinity with the MCF-7 protein for the four compounds, the binding affinity of the synthesized compounds to the protein ranged between (-8.138 _-6.028). C1 had the highest association, as it formed three hydrogen bonds through LEU346, GLU353, and LEU387 and formed Pi-Pi stacking through PHE404, while the binding affinity of C2 formed three hydrogen bonds through GLU353, LEU387, and LEU346. and formed Pi-Pi stacking through PHE404. As for C3, it formed one hydrogen bond through GLU353, p-.pi stacking through PHE404, and a halogen bond through LEU387. And C4 formed three hydrogen bonds through LEU387, GLU353, and LEU346. and formed one Pi-Pi stacking through PHE404.

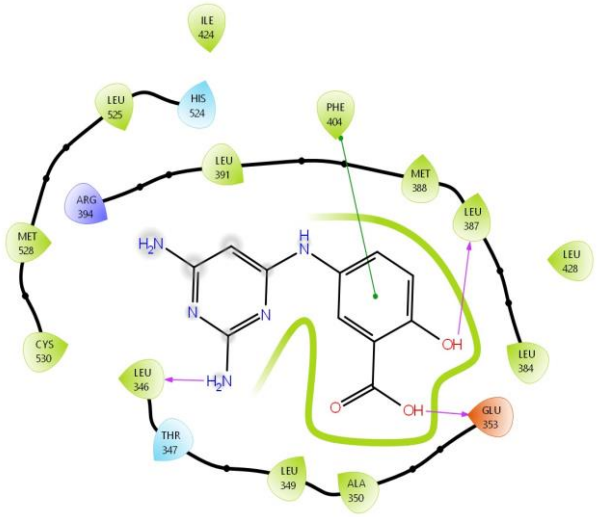

C1

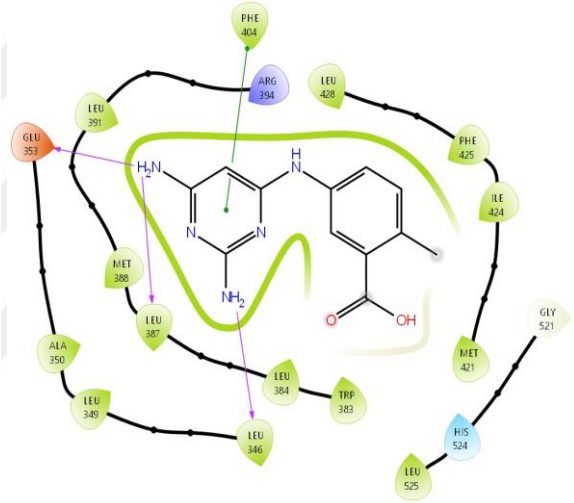

C2

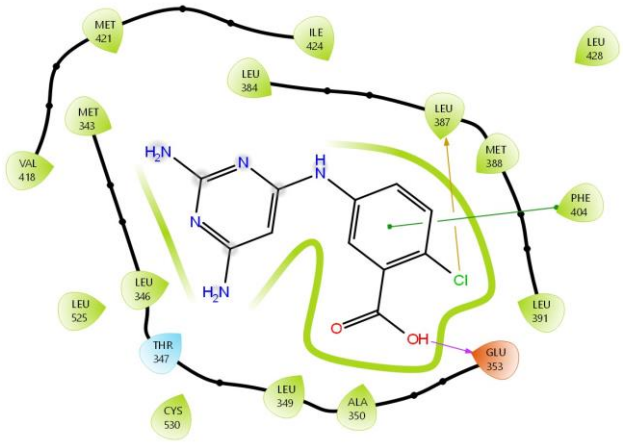

C3

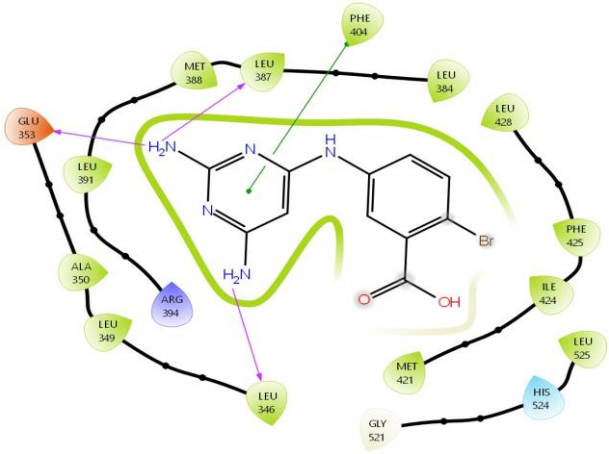

C4

4.2 DFT Analysis

Density functional theory (DFT) encompasses a range of methodologies employed to compute the electronic structures of quantum mechanical systems. Its broad utility extends to both organic and main group compounds, as well as more intricate systems. These methodologies are especially advantageous for studying transition metal complexes, where the influence of electron correlation effects can be substantial. Additionally, they are applicable to systems of similar intricacies, such as metals, solid-state chemicals, and surfaces.[45] Figure (1-4) depicts pictographic representations of C1, C2, C3, and C4 compounds' frontier molecular orbitals. The molecular system's charge distribution is seen in the figures. Positive charge is represented by the green lobes, which are HOMO orbitals, while negative charge is represented by the red lobes, which are LUMO orbitals. The molecular system's HOMO and LUMO distribution over most of the atoms indicated that charge transfer takes place inside the molecule, which might be in charge of the compounds' bioactivity through electronic contact with biological targets.

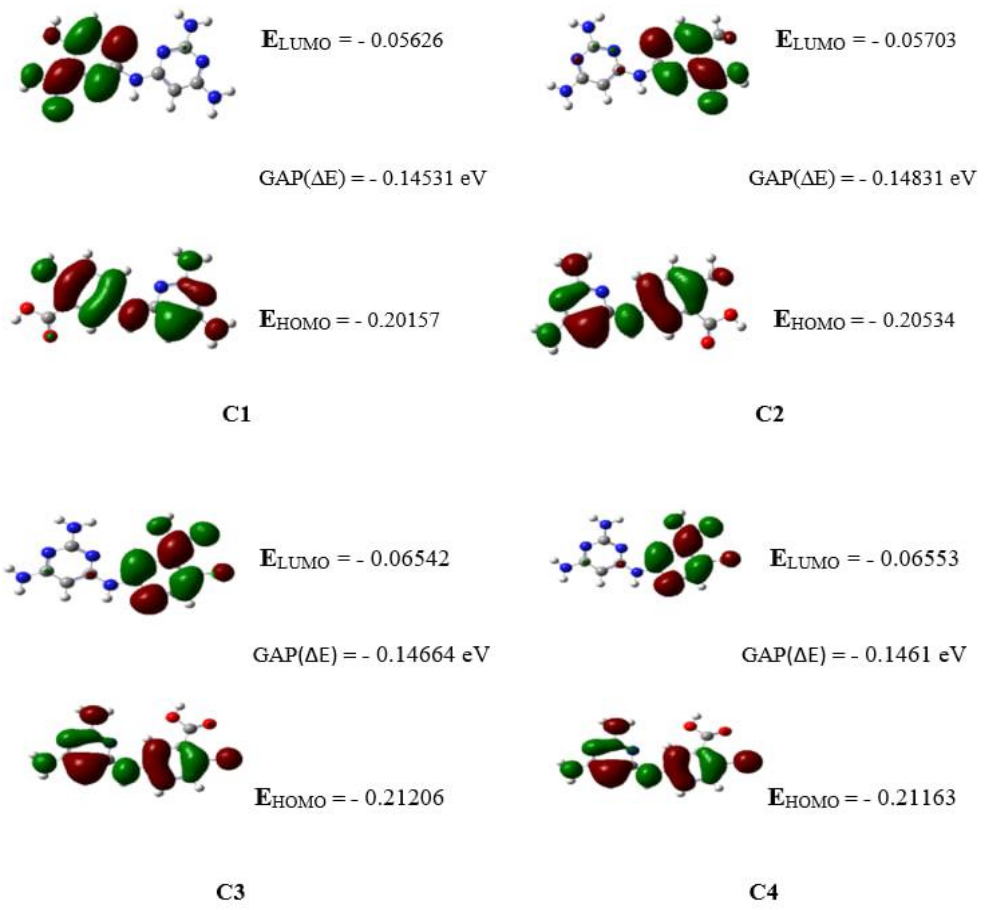

Figure 4-1 HOMO, LUMO and Gap energies for C1, C2, C3 and C4.

All selected molecules had LUMO values ranging from -0.056 to -0.065 eV, HOMO values ranging from -0.20 to -0.21 eV, and Gap values ranging from 0.145 to 0.148 eV. The larger the gap between HOMO and LOMO, the more solid the compounds. Hardness is equal to half the energy gap in terms of numbers. Chemical reactivity generally increases as LUMO energies decrease and HOMO energies increase. Softer chemical species are therefore more reactive than harder ones because they have lower HOMO-LUMO gaps. In terms of quality. This is the capacity of bases or nucleophiles to transfer electrons more easily to acids or electrophiles to start the bond-formation process.[46]

The DFT method specifies basic, universal concepts like the reactivity and stability of molecular structures. To infer the relationships between energy, structure, and reactivity characteristics of complexes, information about IP, EA, electrophilicity index (ω), hardness (η), softness (s), and chemical potential (μ) has

been gathered from the energies of the FMOs, HOMO, and LUMO useful in quantum chemical calculations.[47]

The IP and EA are interpreted as follows: IP = - $\mathbf{E}_{HOMO}$ and EA = - $\mathbf{E}_{LUMO}$. Koopman's theorem is used in the following equations to generate global reactivity descriptors.

The chemical potential (μ) is the tendency of electrons to escape from a stable system. A negative chemical potential indicates a stable complex that does not spontaneously break down into its parts.

$$\mu = -\frac{1}{2}(\mathbf{E}_{HOMO} + \mathbf{E}_{LUMO})$$

Hardness and aromaticity have the same connection. Parr and colleagues, as well as Zhou and Parr, showed that "molecules arrange themselves to be as hard as possible" and that the aromaticity of a range of unsubstituted aromatic compounds may be related to global hardness. A chemical system's hardness indicates its resistance to deformation of its electron cloud under minute stresses.

$$\eta = -\frac{1}{2}(\mathbf{E}_{HOMO} - \mathbf{E}_{LUMO})$$

The interactions between valence shell electrons and the surrounding filled shells and nucleus further influence the electrons' polarizability. Polarizability can be expressed in terms of hardness (η) and softness (S). A large ion that has a small effective nuclear charge and is readily polarized by an external charge is referred to as a soft ion.

$$S = -\frac{2}{(\mathbf{E}_{HOMO} - \mathbf{E}_{LUMO})}$$

The global electrophilicity index (ω) calculates the energy loss owing to maximum electron flow between donor and acceptor using HOMO-LUMO energy values. The determined reactivity descriptor values. The negative chemical potential indicates their stability, implying that they do not decompose into elements.

$$\omega = \frac{\mu 2}{2\eta}$$

Qualities	C1	C2	C3	C4
LUMO	-0.05626	-0.05703	-0.06542	- 0.06553
HOMO	-0.20157	-0.20534	-0.21206	- 0.21163
Gap	-0.14531	-0.14831	-0.14664	- 0.1461
IP	0.20157	0.20534	0.21206	0.21163
EA	0.05626	0.05703	0.06542	0.06553
η	0.072655	0.074155	0.07332	0.07305
μ	0.128915	0.131185	0.13874	0.13858
S	13.76367	13.48526	13.6388	13.6892
ω	0.11430	0.1159	0.13126	0.13144

Table 4-1 Some Chemical properties of the analyzed compounds.

The energy gap values reported in Table (4-1). show that all four compounds C1-C4 have equivalent HOMO-LUMO energy gaps, indicating that the four compounds have comparable chemical reactivity. The lower energy gap between the HOMO and LUMO orbitals suggested that these orbitals might be easily transitioned, resulting in the high reactivity of these compounds. Compound C2 had a smaller energy gap, measuring -0.14831 eV.

4.3 ADMET analysis

4.3.1 Drug-Likeness Criteria

Drug likeness has been frequently employed as a practical criterion for screening compounds in the first phases of drug development. This criterion is developed based on the physicochemical features of authorized medications and prospective drug candidates. The groundbreaking rule of five (Ro5) was applied to evaluate candidates' drug-likeness and minimize the number of submissions. The composition of this entity consists of four distinct criteria, namely molecular mass, the quantity of hydrogen bond donors and acceptors, and logP.[48] According to Lipinski's guidelines, the presence of rotatable bonds (RB) in compounds might potentially impact their oral action and the absorption process of medications (rotatable bonds (RB)<10).[50]

Molecular Mass: According to Lipinski's rule, it is recommended that the molecular masses of medicinal substances be under 500 Daltons.[49] The molecular masses (M. wt. g/mol) of the compounds range from 324.14 to 279.68 All studied derivatives obey this rule.

Lipophilicity (Octanol/water partition coefficient): Lipophilicity, sometimes referred to as Log P, denotes the relative concentration of a molecule in equilibrium between two distinct phases, namely an oil phase and a liquid phase. The consideration of lipophilicity as a physicochemical parameter is imperative in the development of novel pharmaceuticals due to its demonstrated substantial impact on diverse pharmacokinetic characteristics, including absorption, distribution, permeability, and drug clearance pathways. In contrast, it is essential for medicine formulations to possess sufficient water solubility and a suitable level of lipophilicity in order to optimize oral absorption.[51] In Lipinski's rule, log P must not exceed 5.[52] Positive log P values were found for all of the compounds examined, indicating that they exhibit lipophilic properties. all of the compounds obeyed Lipinski's criteria where log P is less than 5 as shown in Table (4-2)

Hydrogen-bond donors and acceptors: The number of hydrogen bonds is an important metric in medication development. Lipinski believes that effective drugs should have 5-10 hydrogen bonds. It must have less than 5 donating bonds (H-BD) between nitrogen-hydrogen and oxygen-hydrogen. Just as the total number of acceptors (H-BA) hydrogen bonds between oxygen and nitrogen is limited to 10, there is an additional restriction stating that the rotatable bonds (RB) are limited to 10. This criterion is obeyed by all studied compounds, indicating that the investigated compounds have effective pharmacological effects. This criterion is obeyed by all studied compounds, indicating that the compounds investigated have effective pharmacological effects.[53] This criterion is obeyed by all studied compounds, indicating that the compounds investigated have effective pharmacological effects.

4.3.2 Human Oral Bioavailability (HOB)

High oral bioavailability is considered to be a crucial pharmacokinetic characteristic of recently discovered drugs, since it falls within the category of ADMET characteristics. The measurement of human oral bioavailability (HOB) is an essential pharmacokinetic parameter used to quantify the amount of medication that reaches the systemic circulation after oral administration. The enhancement of oral bioavailability of the medication might lead to a reduction in adverse effects and concerns regarding toxicity, therefore minimizing the necessary dosage for achieving the desired pharmacological response. In contrast, a low level of oral bioavailability might contribute to the inefficiency of medicine and significant

heterogeneity in its utilization among individuals, hence leading to unforeseen pharmacological consequences.[54] The calculation is built on the presumption that the concentration of the drug in blood or plasma is proportional to its concentration at the action site. Similarly, the compounds were classified based on their percent F values (F% ≤ 50% as "reduced," F% ≥ 50% as "high"). All of the results are shown in Table (4-2), which is considered high based on the F% values, that were greater than 50%.[55]

4.3.3 Human Intestinal Absorption (HIA)

Preclinical ADMET screening techniques are regarded as a key tool for identifying compounds as prospective therapeutic candidates early in the drug development process. Human Intestinal Absorption (HIA) is an important ADMET property because it is one of the key steps in medication transport to their destinations.[56] HIA was categorized into three parts: high (100–67%), middle (66–33%), and low (32–0%).[57] The compounds exhibited a HIA examined ranged from 96.55% to 98.27%. This observation typically suggests that these compounds had the potential for oral administration.

Qualities	C1	C2	C3	C4
M. Wt.	261.24	259.27	279.69	324.14
Alog P	0.79	1,39	1.74	1,85
H-BA	7	6	6	6
H-BD	5	4	4	4
RB	3	3	3	3
HIA	98.27%	97.97%	97.10%	96.55%
HOB	57.14%	74.%29	78.57%	78.57%

Table 4-2 ADMET Predictions of studied compounds.

4.4 Characterization of Synthetic derivative

4.4.1 General Characteristics

The solvents used in the preparation: Distilled Water, purple powdery product of C1, Chemical Formula: $C_{11}H_{11}N_5O_3$, beige powdery product of C2, Chemical Formula: $C_{12}H_{13}FN_5O_2$, White to light yellow powdery product of C3, Chemical Formula: $C_{11}H_{10}ClN_5O_2$, white crystalline solid product of C4, Chemical Formula: $C_{11}H_{10}BrN_5O_2$. Form crystalline products was noticed more clearly with the ethanol solvent.

4.4.2 Melting Points

Melting points (m.p) of the synthetic compounds are measured, and the degrees were as shown in Table (4-3).

Compounds	C1	C2	C3	C4
m.p °C	310-315 °C	335-338 °C	320-225°C	330-334°C

Table 4-3 m.p of synthetic compounds.

4.4.3 Solubility in Different Solvents

The Solubility of the synthetic compounds in several solvents with different polarity was tested, and the results are shown in Table (4-4).

solvents	C1	C2	C3	C4
Distilled water	-	-	-	-
Ethanol	-	-	-	-
Methanol	-	-	-	-
Benzene	-	-	-	-
Hexane	-	-	-	-
DMF	-	-	-	-
DMSO	+	+	+	+

Table 4-4 Solubility of synthetic compounds.

4.4.4 Spectroscopic Analysis

4.4.4.1 C1 Characterization

4.4.4.1.1 IR spectrum: The synthesis of the selected C1 was demonstrated by IR spectroscopic analysis, which revealed significant absorption bands. Firstly, broad and strong band between 2800-3500 cm^{-1} belonging to the carboxyl group stretching, medium band at 3320 cm^{-1} to belongs to the NH stretching, medium 3126 cm^{-1} to O-H strectcing , strong band at 1668 cm^{-1} to C=O group, medium band at 1623 cm^{-1} to C=C aromatic, weak band at 1555 cm^{-1} to N-H bending, strong band at 1455 cm^{-1} to C-N stretching, and strong band at 1237 cm^{-1} to C-O group as shown in Figure (4-2).

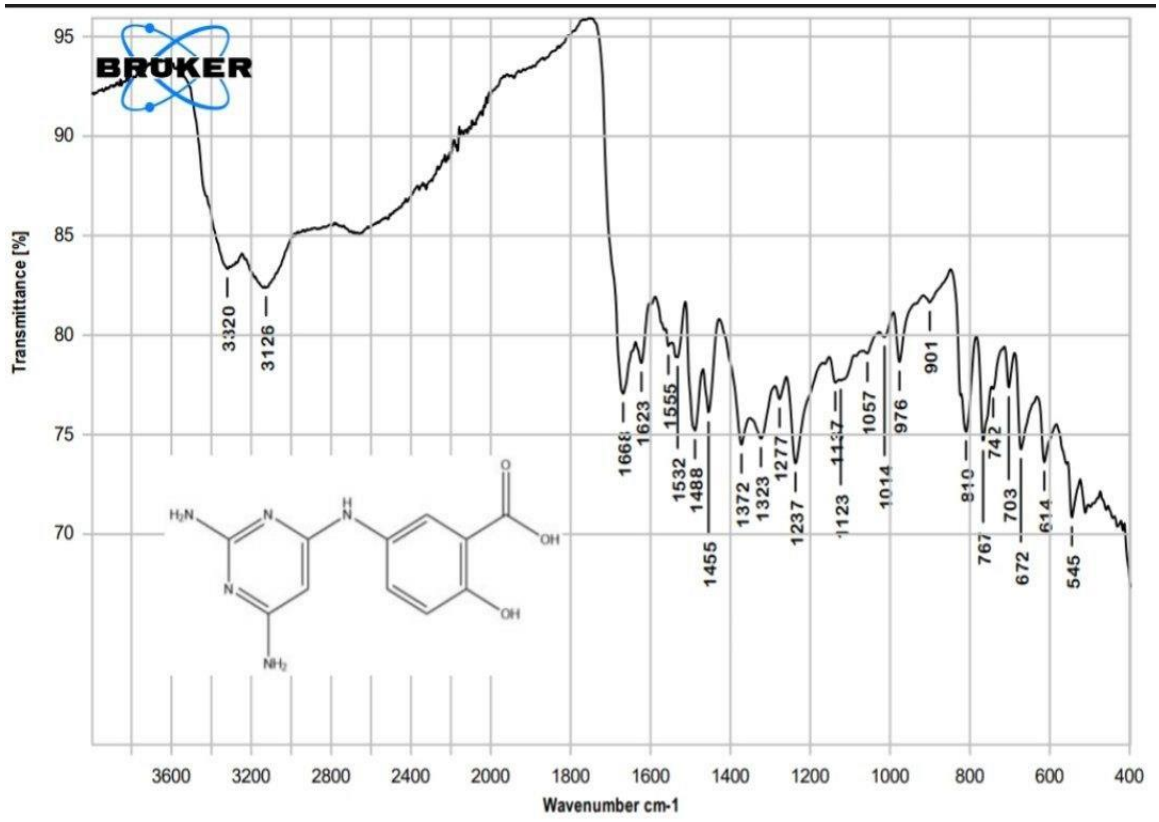

Figure 4-2 Infrared spectrum of C1.

4.4.4.1.2 ^{1}H-NMR Spectrum: The synthesized compounds were characterized using ^{1}H-NMR and ^{13}C-NMR spectroscopy; chemical shifts are given in ppm (δ) relative to TMS. Multiplet, singlet, doublet, triplet, and quartet are denoted by the letters m, s, d, t, and q, respectively. The signals of C1 protons are: (500 MHz, DMSO) δ 9.36 (s, ^{1}H), 7.72 (d, ***J*** = 2.9 Hz, ^{1}H), 7.55 (s, ^{2}H), 7.37 (s, ^{1}H), 7.34 (s, ^{2}H), 6.80 (d, ***J*** = 8.7 Hz, ^{1}H), 5.15 (s, ^{1}H). All Signals shown in Figure (4-3).

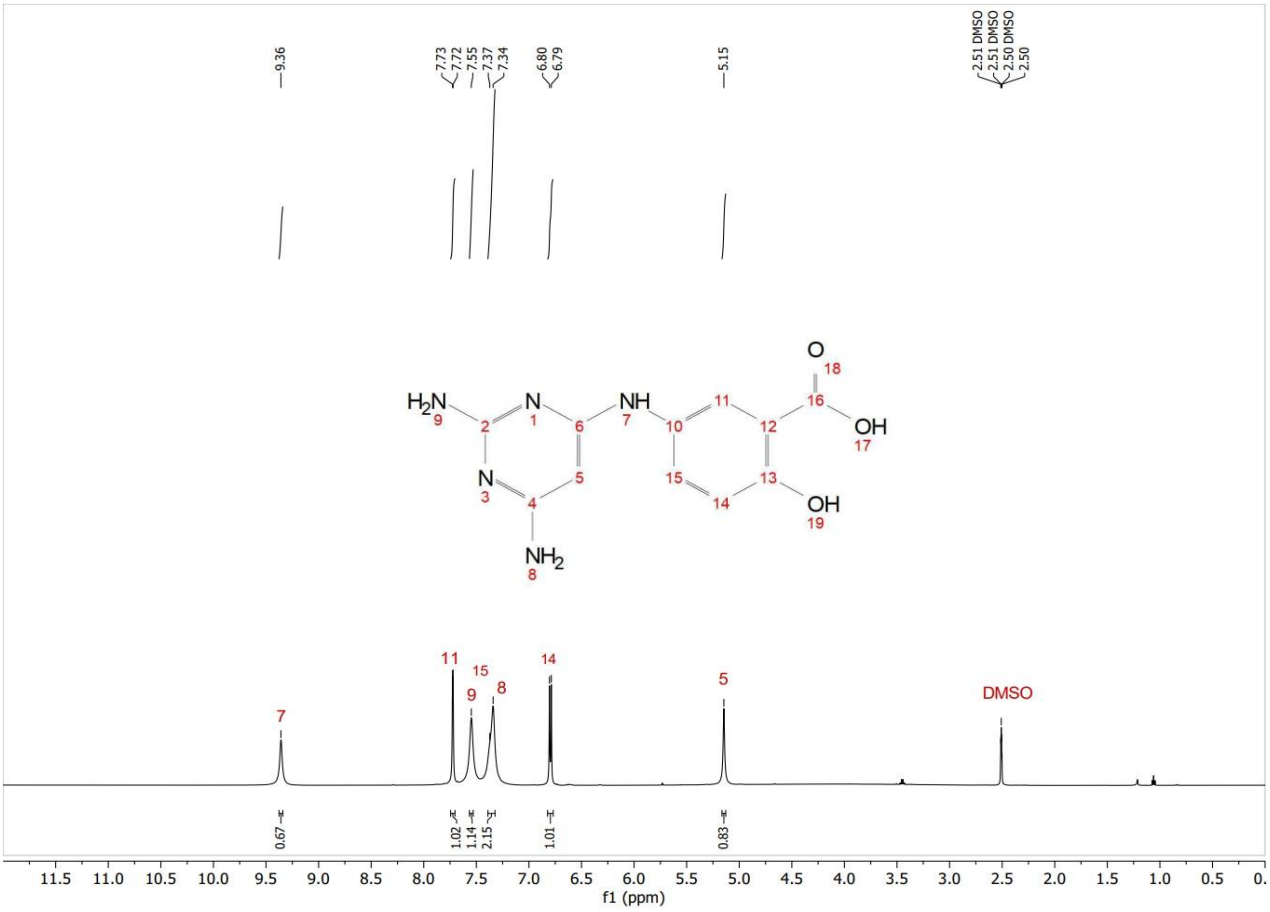

Figure 4-3 ^{1}H-NMR spectroscopy of C1.

4.4.4.1.3 ^{13}C-NMR Spectrum: The ^{13}C-NMR (125 MHz, DMSO) spectrum of compound C1 taken from its DMSO solution shows the signals:: (125 MHz, DMSO) δ 173.27, 161.75, 159.59, 155.35, 129.58, 128.34, 126.58, 119.44, 116.98, 73.4 and 56.54 ppm. which are assigned to their carbon atoms as shown in Figure(4-4).

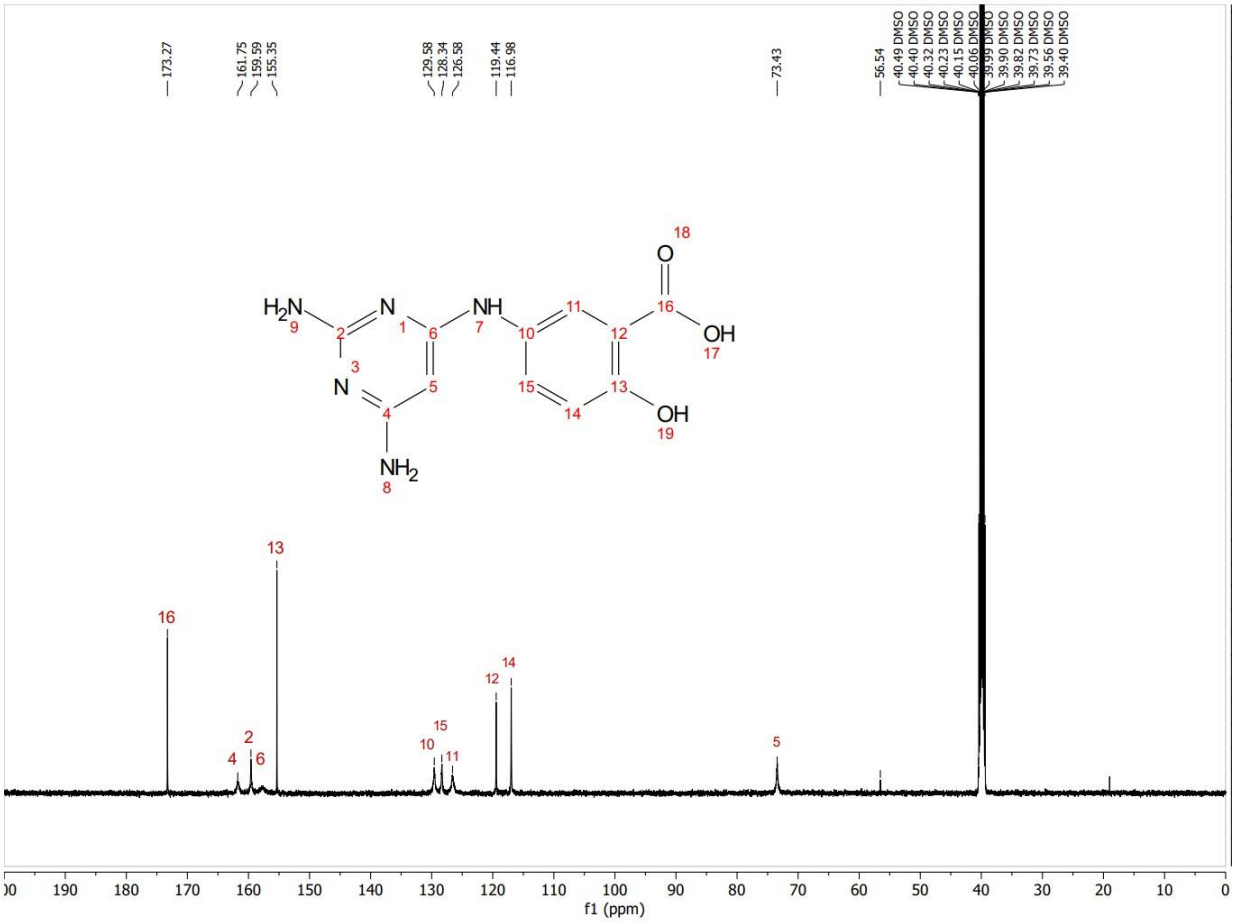

Figure 4-4 ^{13}C-NMR spectroscopy of C1 taken from DMSO solution.

4.4.4.1.4 LC-Mass Spectrum: C1 spectrum was shown in Figure (4-5), the M. wt peak for $C_{11}H_{11}N_5O_3$ equals 262.40 m/z, which was very much nearly with the theoretical value.

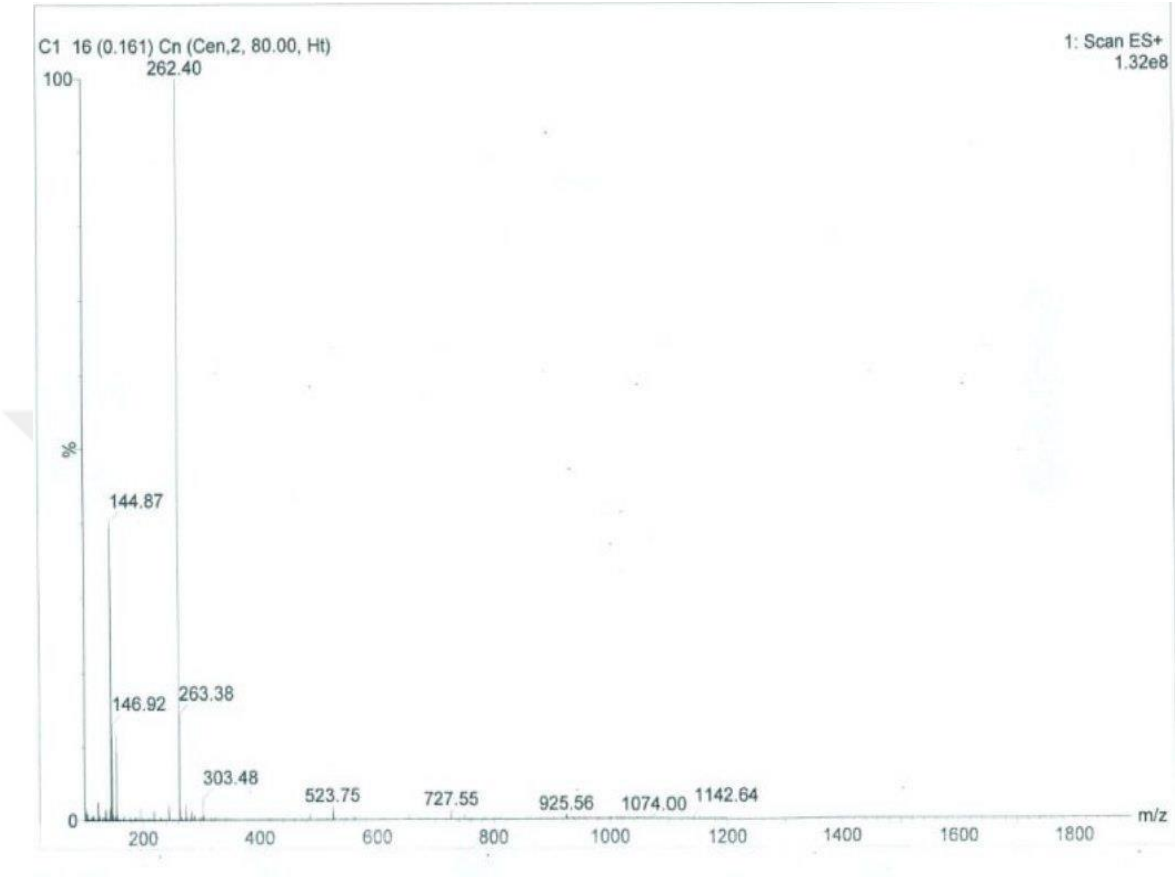

Figure 4-5 LC-MS spectroscopy of C1.

4.4.4.2 C2 Characterization

4.4.4.2.1 IR Spectrum: The synthesis of the selected C2 was demonstrated by IR spectroscopic analysis, which revealed significant absorption bands. Firstly, broad and very strong band between 2800-3500 cm^{-1} belonging to the carboxyl group, medium band at 3470-3417 cm^{-1} to NH stretch, medium band at 3311 cm^{-1} to O-H carboxyl group, strong band at 1645 cm^{-1} to C=O group, medium band at 1588 cm^{-1} to C=C aromatic, medium band at 1547 cm^{-1} to N-H bending, medium band at 1370 cm^{-1} to CH_3 group and strong band at 1294 cm^{-1} to C-O group as shown in Figure (4-6).

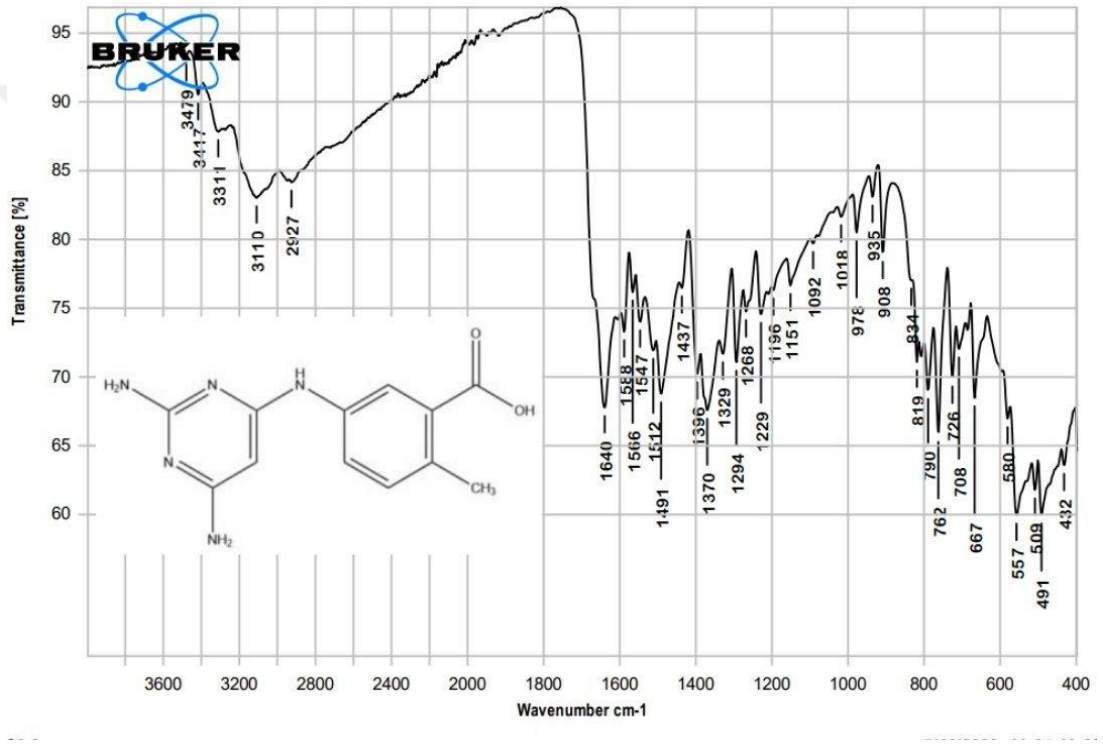

Figure 4-6 Infrared spectrum of C2.

4.4.4.2.2 ^{1}H-NMR Spectrum: The synthesized compounds were characterized using ^{1}H-NMR and ^{13}C-NMR spectroscopy; chemical shifts are given in ppm (δ) relative to TMS. Multiple, singlet, doublet, triplet, and quartet are denoted by the letters m, s, d, t, and q, respectively. The signals of C2 protons are; (500 MHz, DMSO) δ 8.58 (s, 1H), 7.88 (dd, *J* = 8.3, 2.5 Hz, 1H), 7.74 (d, *J* = 2.4 Hz, 1H), 7.12 (d, *J* = 8.4 Hz, 1H), 5.89 (s, 2H), 5.70 (s, 2H), 5.18 (s, 1H), 2.43 (s, 3H), 2.41 (s, 1H) as shown in Figure (4-7).

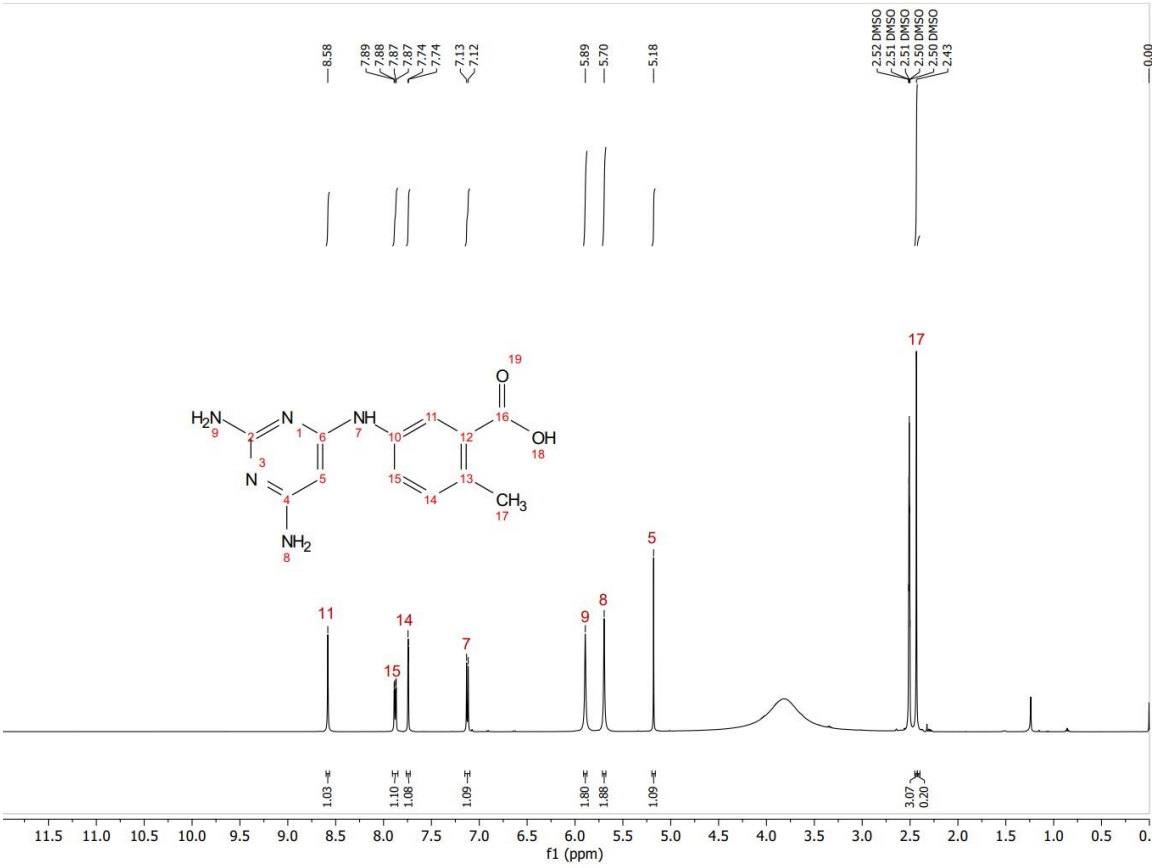

Figure 4-7 ^{1}H-NMR spectroscopy of C2.

4.4.4.2.3 ^{13}C-NMR Spectrum: The ^{13}C-NMR (125 MHz, DMSO) spectrum of compound C2 taken from its DMSO solution shows the signals: NMR δ 169.70, 164.51, 162.74, 161.93, 139.60, 131.96, 131.55, 131.23, 123.27, 121.58, 76.59 and 21.0 ppm. which are assigned to their carbon atoms as shown in Figure (4-8).

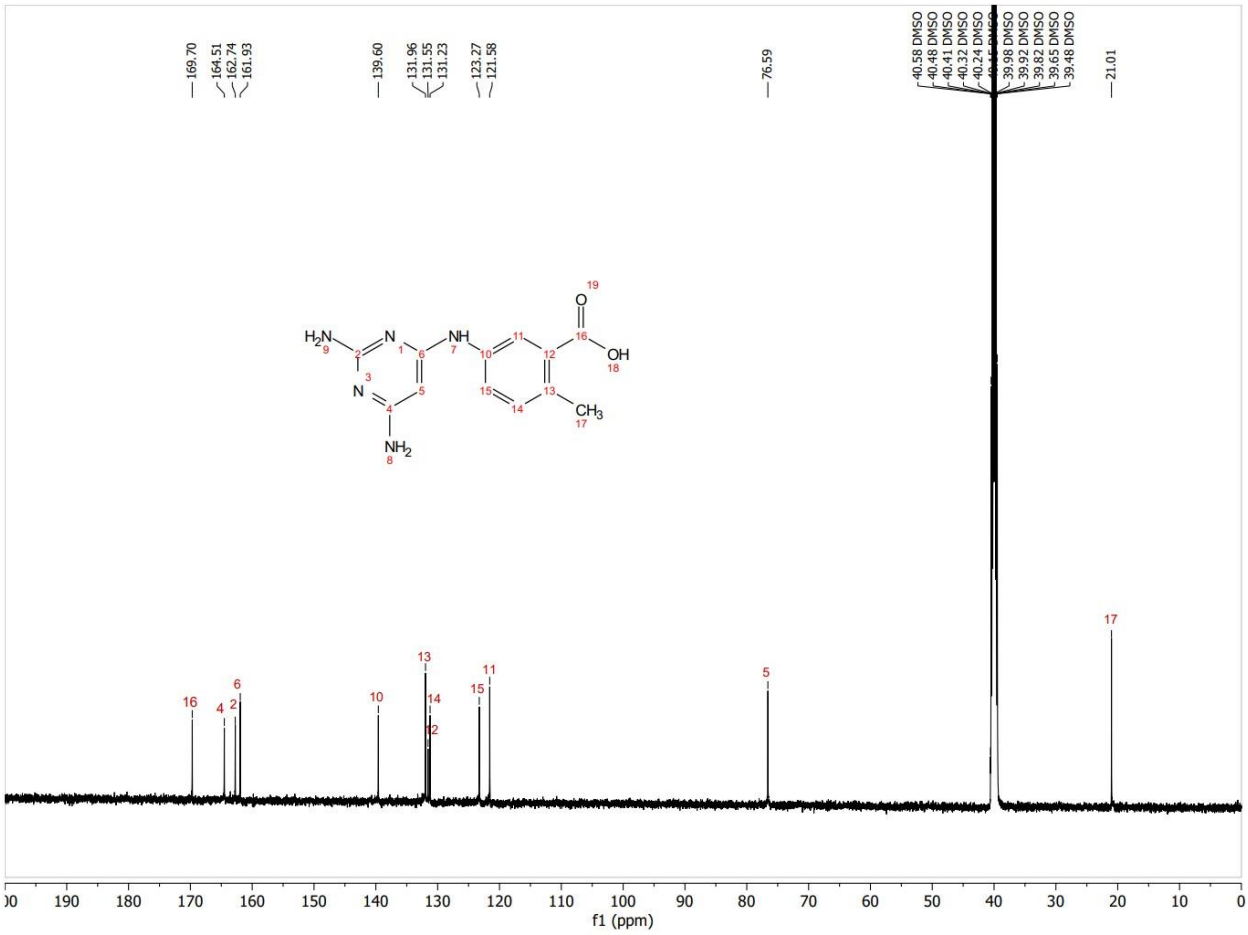

Figure 4-8 ^{13}C-NMR spectroscopy of C2 taken from DMSO solution.

4.4.4.2.4 LC-Mass Spectrum: The C2 spectrum is shown in Figure (4-9), the M. wt peak for $C_{12}H_{13}N_5O_2$ equals 260.41 m/z, which was very much nearly to the theoretical value.

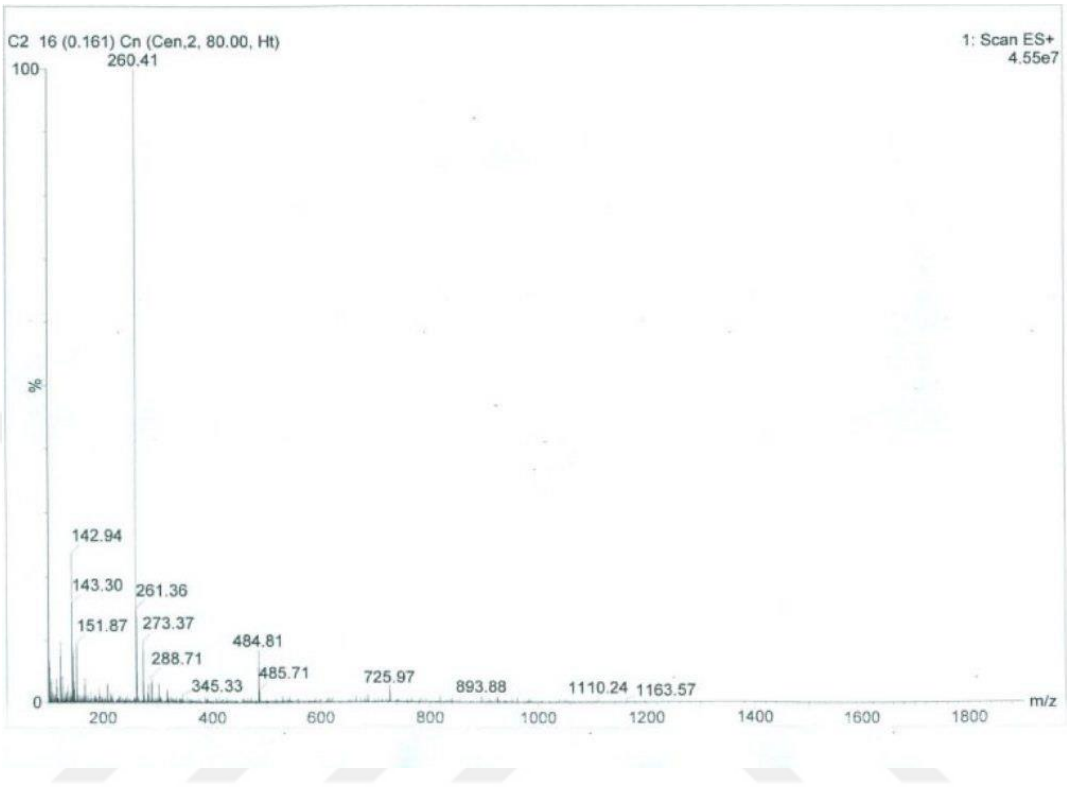

Figure 4-9 LC-MS spectroscopy of C2.

4.4.4.3 Characterization

4.4.4.3.1 IR Spectrum: The synthesis of the selected C3 was demonstrated by IR spectroscopic analysis, which revealed significant absorption bands Firstly, broad and very strong bands between 2800-3600 cm^{-1} to the carboxyl group, medium 3486–3414 cm^{-1} to the N-H stretch, medium 3138 cm-1 to the O-H carboxyl group, medium 2952 cm^{-1} to the C-H stretch, strong 1644 cm^{-1} to the C=O group, medium 1591 cm^{-1} to the C=C aromatic, medium 1519 cm^{-1} to the N-H bending, strong 1294 cm^{-1} to the C-O group, strong 1045 cm^{-1} to the C-N, and strong 763 cm^{-1} to the C-Cl group, as shown in Figure (4-10).

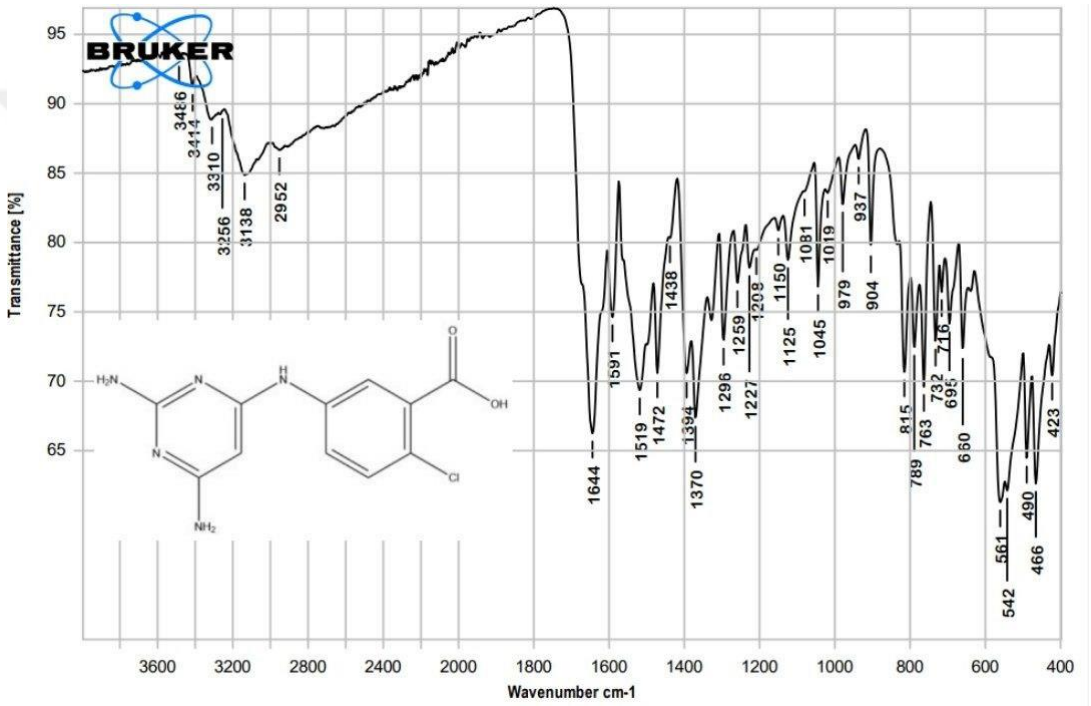

Figure 4-10 Infrared spectrum of C3.

4.4.4.3.2 ^{1}H-NMR Spectrum: The synthesized compounds were characterized using ^{1}H-NMR and ^{13}C-NMR spectroscopy; chemical shifts are given in ppm (δ) relative to TMS. Multiplet, singlet, doublet, triplet, and quartet are denoted by the letters m, s, d, t, and q, respectively. The Signals of C3-Protons are; (500 MHz, DMSO) δ 8.91 (d, J = 3.4 Hz, 1H), 7.98 (dd, J = 8.8, 2.7 Hz, 1H), 7.78 (d, J = 2.8 Hz, 1H), 7.31 (d, J = 8.9 Hz, 1H), 6.09 (s, 2H), 5.94 (s, 2H), 5.20 (s, 1H). as shown in Figure (4-11).

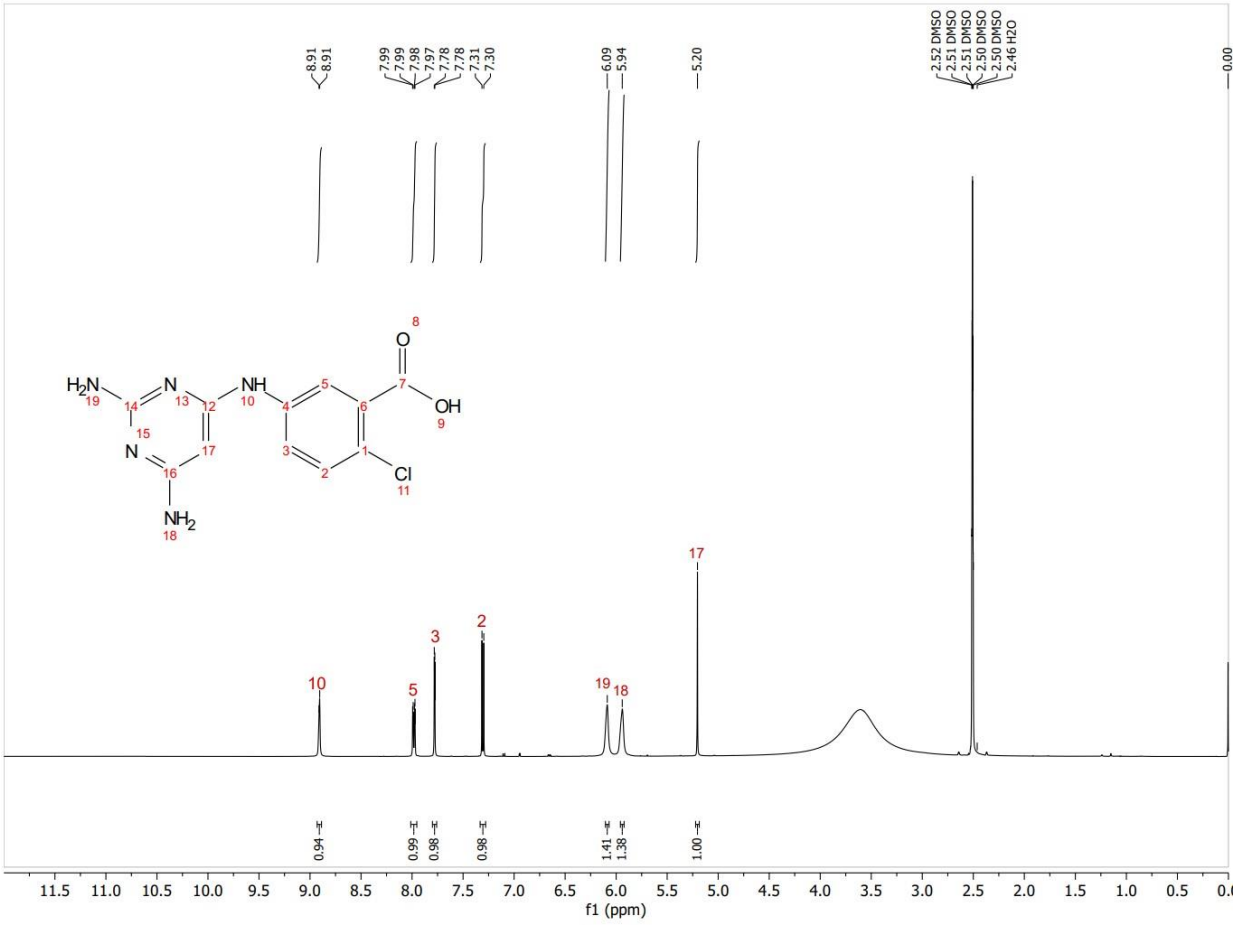

Figure 4-11 ^{1}H-NMR spectroscopy of C3.

4.4.4.3.3 ^{13}C-NMR Spectrum: The ^{13}C-NMR (125 MHz, DMSO) spectrum of C3 shows the appearance of the following signals : δ 167.77, 164.27, 162.45, 161.53, 140.96, 132.74, 130.78, 122.65, 122.40, 120.82 and 77.27 ppm. Which are assigned to their carbon atoms as shown in Figure (4-12).

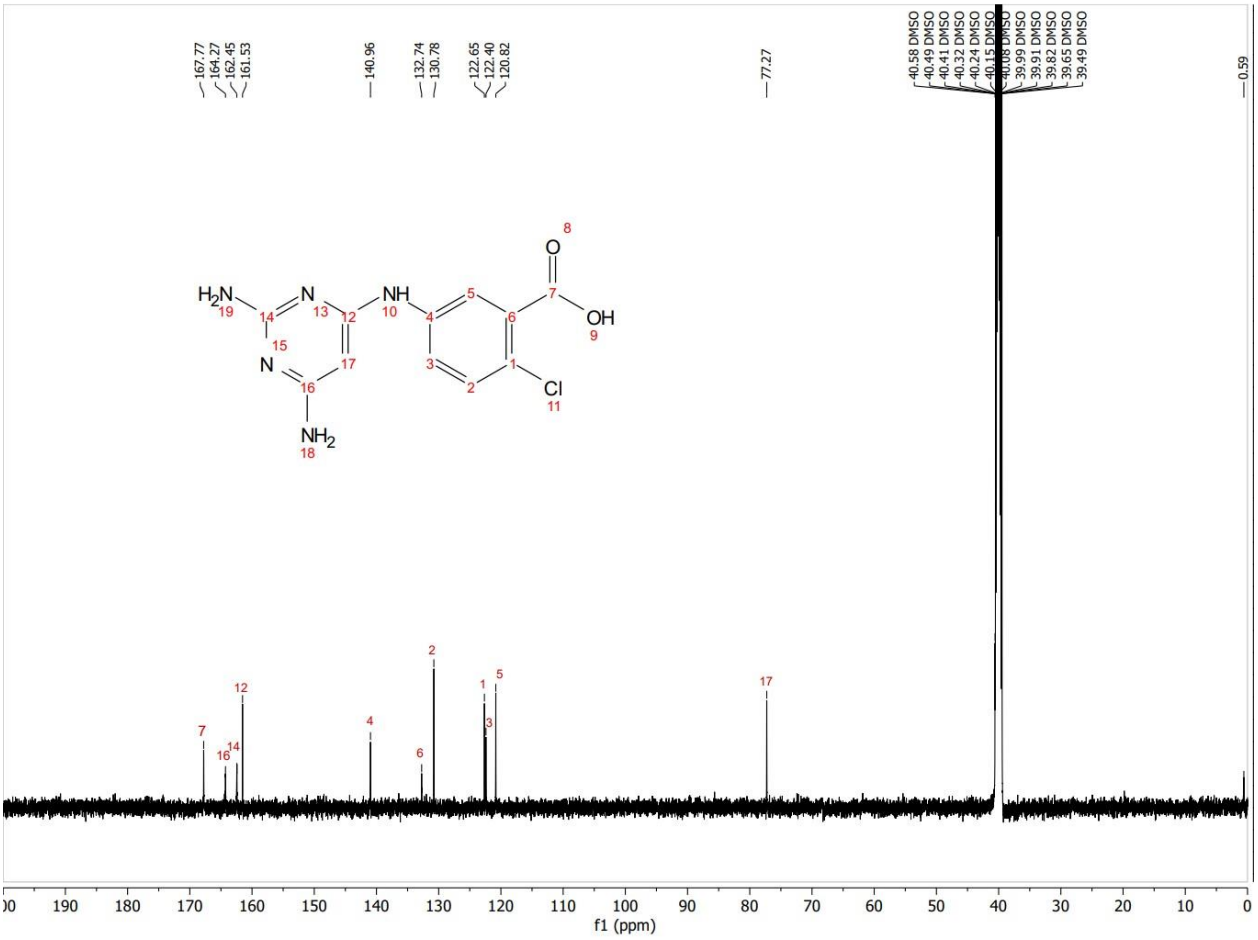

Figure 4-12 ^{1}H-NMR spectroscopy of C3.

4.4.4.3.4 LC-Mass Spectrum: The C3 spectrum is shown in Figure (4-13), the M. wt peak for $C_{11}H_{10}ClN_5O_2$ equals 280.44 m/z, which was very much nearly to the theoretical value.

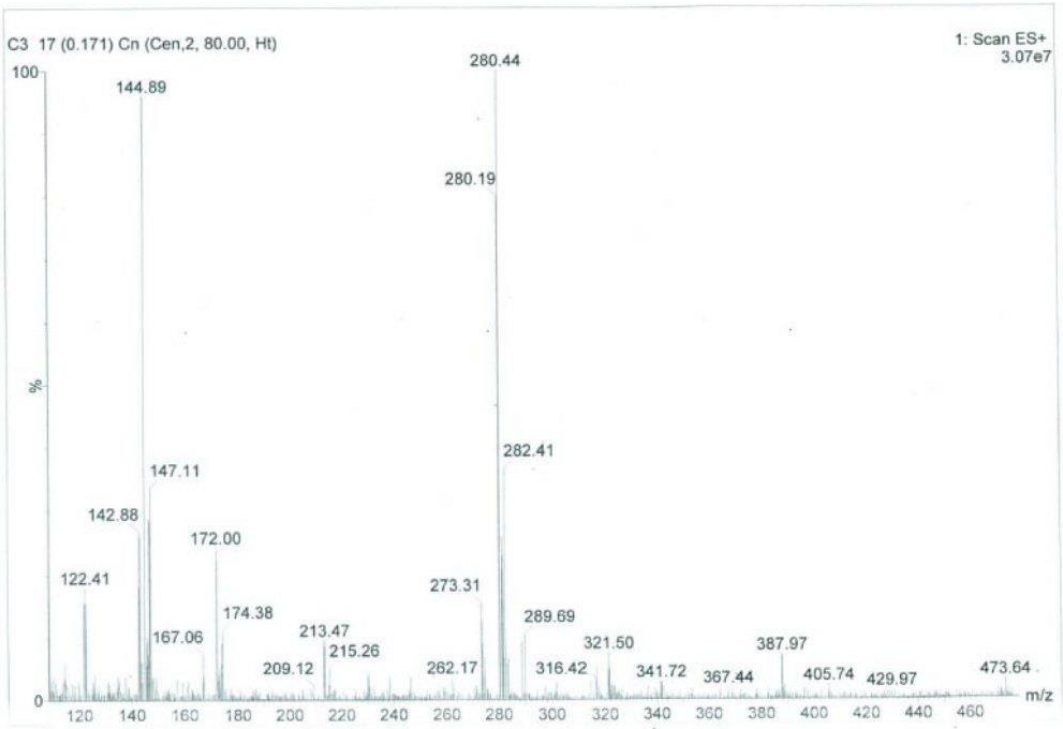

Figure 4-13 LC-MS spectroscopy of C3.

4.4.4.4 C4 Characterization

4.4.4.4.1 IR Spectrum: The synthesis of the selected C4 was demonstrated by IR spectroscopic analysis, which revealed significant absorption bands. Firstly, a broad and very strong band between 2800–3500 cm^{-1} carboxyl group, medium 3414–3309 cm^{-1} to N-H stretch, medium 3137 cm^{-1} to O-H carboxyl group, strong 1645 cm^{-1} to C=O group, medium 1618 cm^{-1} to C=C aromatic, strong 1524 cm^{-1} to N-H bending, strong 1296 cm^{-1} to C-N stretching, strong 1028 cm^{-1} to C-O group, and strong 763 cm^{-1} to C-Br group, as shown in Figure (4-14).

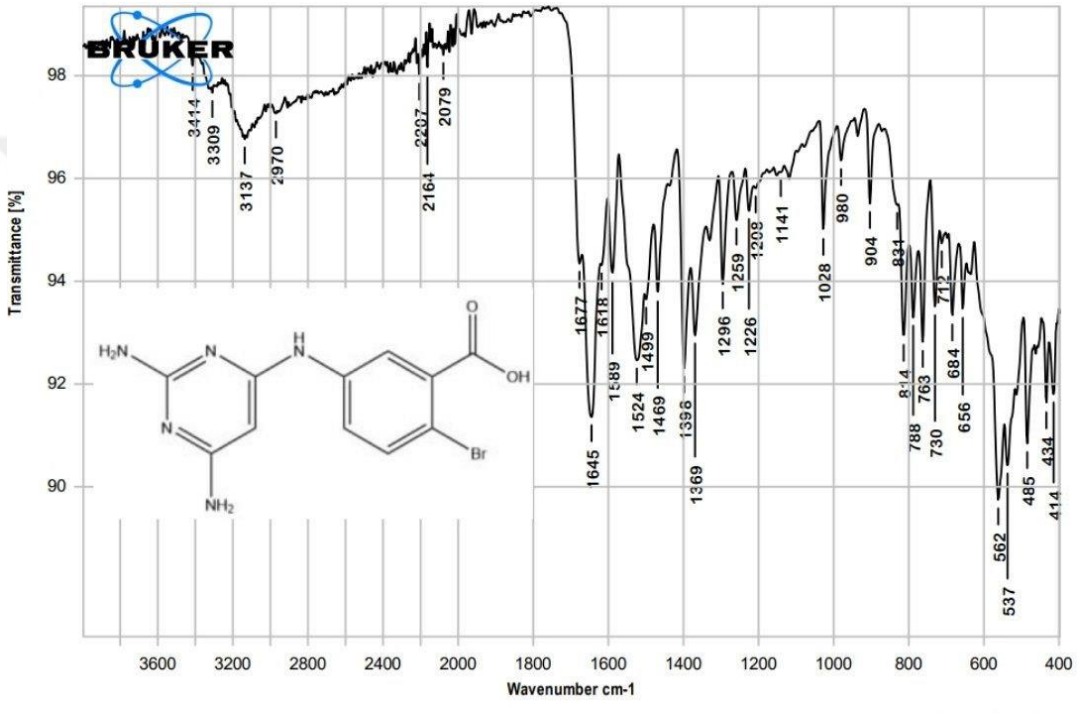

Figure 4-14 Infrared spectrum of C4.

4.4.4.4.2 ^{1}H-NMR Spectrum: The synthesized compounds were characterized using ^{1}H-NMR and ^{13}C-NMR spectroscopy; chemical shifts are given in ppm (δ) relative to TMS. Multiple, singlet, doublet, triplet, and quartet are denoted by the letters m, s, d, t, and q, respectively. Signals of C4; (500 MHz, DMSO) δ 8.91 (d, J = 2.3 Hz, 1H), 7.89 (dd, J = 8.8, 2.7 Hz, 1H), 7.77 (d, J = 2.7 Hz, 1H), 7.46 (d, J = 8.8 Hz, 1H), 6.10 (s, 1H), 5.94 (d, J = 5.5 Hz, 2H), 5.21 (s, 1H), 2.47 (s, 1H), 2.35 (s, 2H).as shown in Figure (4-17).

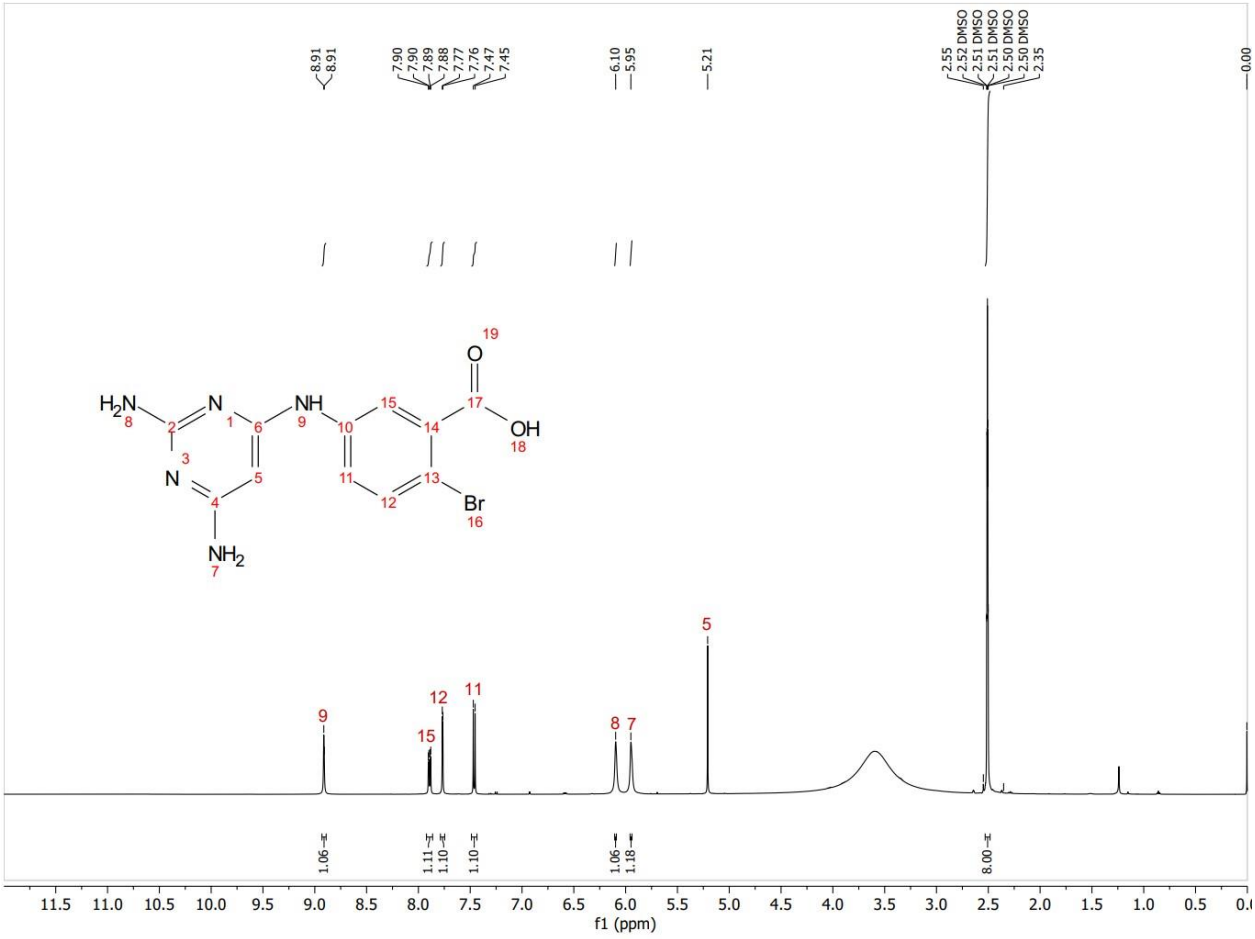

Figure 4-15 ^{1}H-NMR spectroscopy of C4.

4.4.4.4.3 ^{13}C-NMR Spectrum: The ^{13}C-NMR (125 MHz, DMSO) spectrum of C4 shows the appearance of the following signals δ 168.43, 164.16, 162.33, 161.50, 141.45, 135.08, 133.87, 122.72, 120.77, 110.04, and 77.31ppm. Which are assigned to their carbon atoms as shown in Figure (4-16).

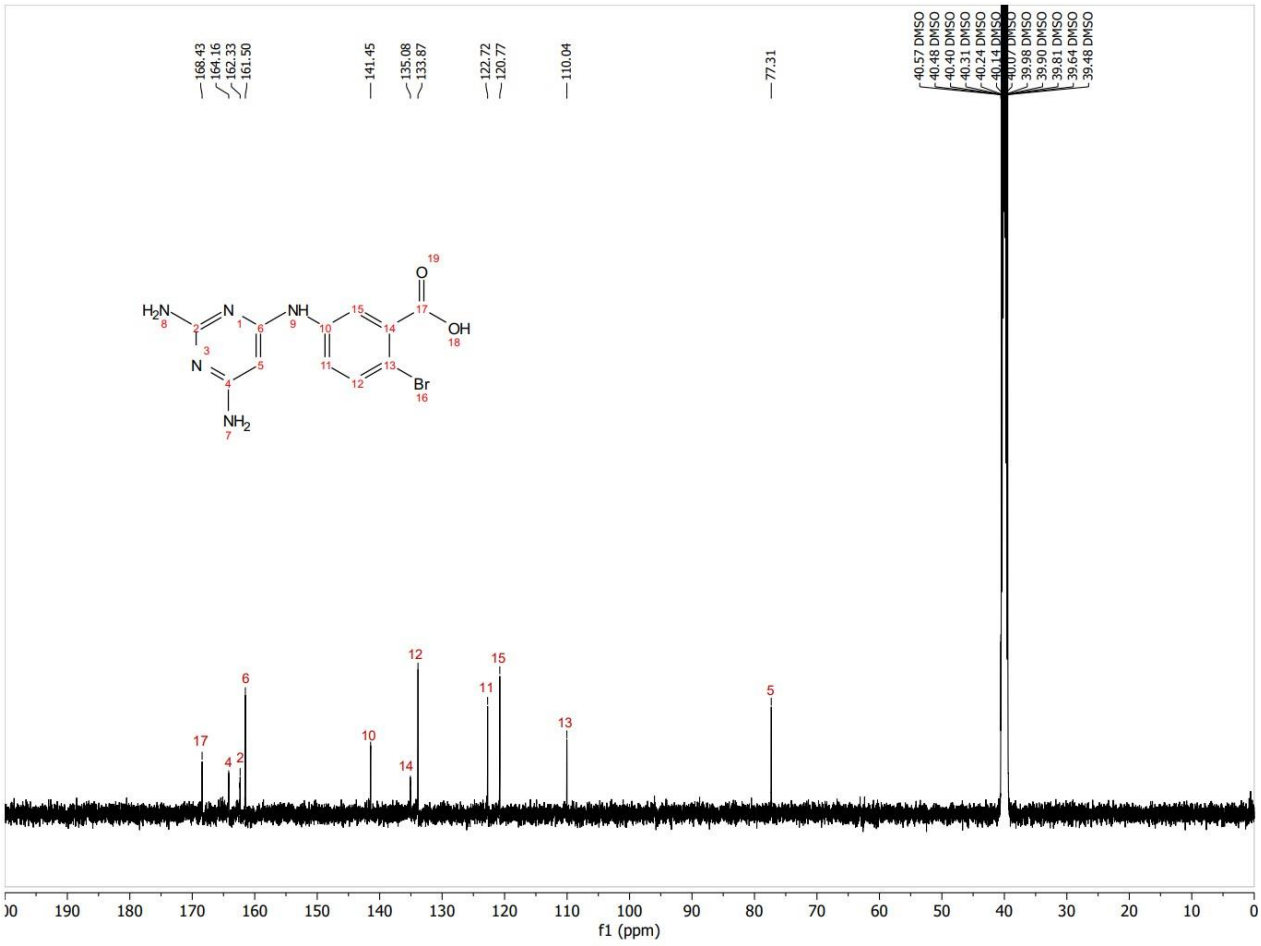

Figure 4-16 ^{13}C-NMR spectroscopy of C4 taken from DMSO solution.

4.4.4.4.4 LC-Mass Spectrum: The C4 spectrum is shown in Figure (4-17), the M. wt peak for $C_{11}H_{10}BrN_5O2$ equals 324.51 m/z, which was very much nearly to the theoretical value.

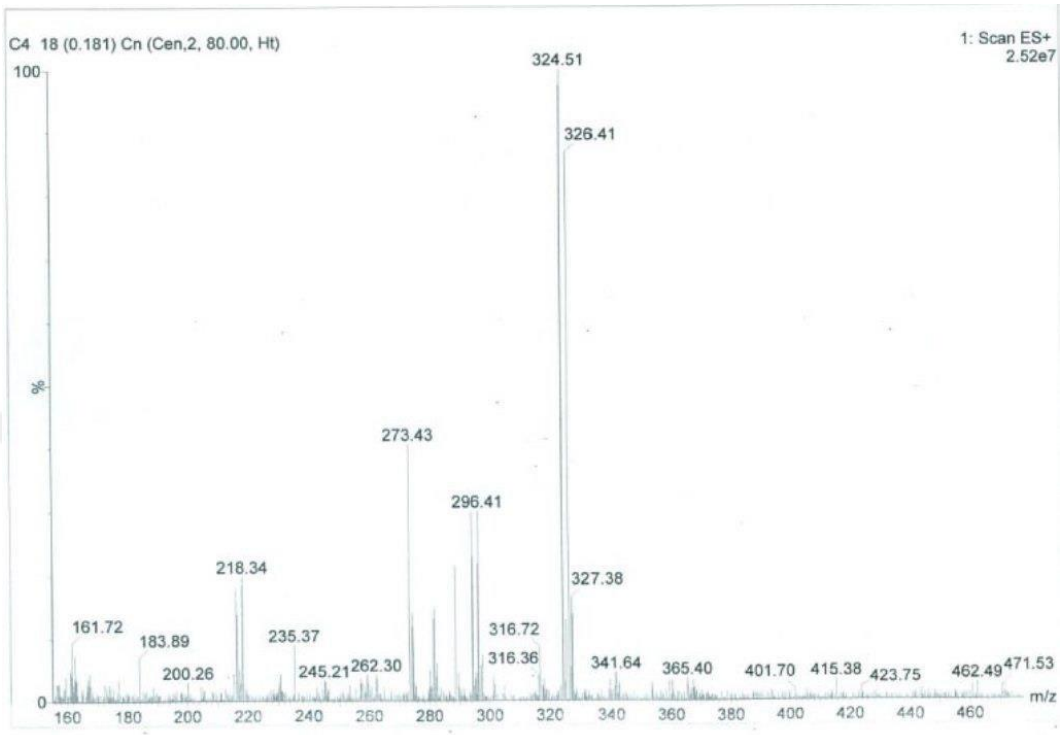

Figure 4-17 LC-MS spectroscopy of C4.

4.5 Biological Activity and Inhibitory Effect

The MTT assay is a commonly employed technique for initial screening purposes in order to identify compounds with potential anticancer properties. Additionally, this assay allows for the assessment of morphological alterations in cells, thereby enabling the evaluation of cytotoxic effects exhibited by synthesized compounds. In this study, the cytotoxic activities of the synthesized compounds were examined against two specific cancer cell lines, mammary gland breast cancer (MCF-7) and colorectal carcinoma (HCT-116). The MTT assay was utilized, with Doxorubicin serving as a reference anticancer agent. Table (4-5) displays the findings of the initial assessment conducted to determine the antiproliferative effects. The cytotoxicity assay findings indicated that the majority of the synthesized compounds exhibited moderate to high cytotoxic activity against the chosen two cancer cell lines. The concentrations required to achieve a 50% inhibition of tumor cell growth were determined for the target chemicals.

Compound	MCF-7	HCT-116
C1	19.15 ± 1.01	11.89 ± 1.02
C2	12.34 ± 0.73	10.29 ± 0.23
C3	16.76 ± 0.73	8.17 ± 0.45
C4	10.89 ± 1.23	14.32 ± 1.10
Doxorubicin	6.39 ± 0.23	5.22 ± 0.50

Table 4-5 In vitro anticancer activity of the designed compounds.

5. CONCLUSIONS AND RECOMMENDATIONS

5.1 CONCLUSIONS

1. The prediction of the theoretical study for 4 compounds (C1, C2, C3 and C4) as drug-likeness compounds with anti-cancer activity. The results show that Compound C1 exhibits the highest binding affinity towards mammary gland breast cancer (MCF-7) and compound C4 towards colorectal carcinoma (HCT-116).
2. The measurements of HOMO, LUMO, and GAP indicate that molecules exhibit a preference for behaving as acids rather than bases. Additionally, these compounds demonstrate high kinetic activity but relatively poor stability.
3. The ADMET Prediction Results validate the Compliance of the compounds with the pharmaceutical standards.
4. The effectiveness of the synthesis approach employed in the production of compounds C1, C2, C3, and C4 was established by chemical characterization using techniques such as infrared spectroscopy (IR), proton nuclear magnetic resonance spectroscopy (^{1}H-NMR), carbon-13 nuclear magnetic resonance spectroscopy (^{13}C-NMR), and liquid chromatography-mass spectrometry (LC-MS) measurements.
5. Finally, the synthesized compounds showed acceptable inhibitory activity, that makes them to be considered for future therapeutic alternatives after a deep pharmaceutical evaluation study.

5.2 RECOMMENDATIONS

Through the results obtained in this study, we recommend:

1. A comprehensive examination of the possible anticancer properties of all produced substances through in vivo experimentation.
2. Synthesis of C1, C2, C3, and C4 compounds that are expected to give higher anticancer activity than those synthesized in this research .
3. In vitro evaluation of newly synthetic compounds to determine the potential clinical therapeutic.
4. Conducting out additional ADMET prediction measurements on the investigated compounds to theoretically uncover more of their therapeutic properties.

6. REFERENCES

"Vancouver citation system was used in this thesis"

1. *Snyder IS, Janet L. Anticancer Drug. Encycl. Br.*
2. *Albratty M, Alhazmi HA. Novel pyridine and pyrimidine derivatives as promising anticancer agents: A review. Arabian Journal of Chemistry. 2022 Jun 1;15(6):103846.*
3. *Vorontsov AV, Smirniotis PG. Advancements in hydrogen energy research with the assistance of computational chemistry. International Journal of Hydrogen Energy. 2023 Jan 21.*
4. *. Metin M, Kawano T, Okobira T. Nitrogen as a probable problematic factor of computational chemistry: A benchmarking study. Journal of the Indian Chemical Society. 2023 Jul 1;100(7):101030*
5. *Mammino L. Green chemistry and computational chemistry: a wealth of promising synergies. Sustainable Chemistry and Pharmacy. 2023 Sep 1;34:101151.*
6. *He L, Bai L, Dionysiou DD, Wei Z, Spinney R, Chu C, Lin Z, Xiao R. Applications of computational chemistry, artificial intelligence, and machine learning in aquatic chemistry research. Chemical Engineering Journal. 2021 Dec 15;426:131810.*
7. *Polanski J. Chemoinformatics in: Comprehensive Chemometrics. Polanski, J., Brown, SD, Tauler, R., Walczak, B., Eds. 2009:459-506.*
8. *Pandey A, Tiwari B, Pandey A, Yusup S, editors. Current Developments in Biotechnology and Bioengineering: Deep Eutectic Solvents: Fundamentals and Emerging Applications.*
9. *Maffucci I, Contini A. Tuning the solvation term in the MM-PBSA/GBSA binding affinity predictions. InFrontiers in Computational Chemistry 2015 Jan 1 (pp. 82-120). Bentham Science Publishers.*
10. *Hu M. Computational modeling of thermal transport in bulk and nanostructured energy materials and systems. InModeling, Characterization, and Production of Nanomaterials 2023 Jan 1 (pp. 151-170). Woodhead Publishing*
11. *Tuckerman ME, Martyna GJ. Understanding modern molecular dynamics: Techniques and applications. The Journal of Physical Chemistry B. 2000 Jan 20;104(2):159-78.*
12. *Barbhuiya S, Das BB. Molecular dynamics simulation in concrete research: A systematic review of techniques, models and future directions. Journal of Building Engineering. 2023 Jul 3:107267.*
13. *Liu Z, Xie Z, Dong W, Yuan M, You H, Li D. A heterogeneous processing-in-memory approach to accelerate quantum chemistry simulation. Parallel Computing. 2023 Jul 1;116:103017.*
14. *Wu X, Su P. Very brief introduction to quantum chemistry. InQuantum Chemistry in the Age of Machine Learning 2023 Jan 1 (pp. 3-25). Elsevier.*
15. *Yang S, Wang Y, Liu ZK, Zhong Y. Ab initio studies on structural and thermodynamic properties of magnetic Fe. Computational Materials Science. 2023 Aug 1;227:112299.*
16. *Marqués LA, Aboy M, López P, Santos I, Pelaz L, Fisicaro G. Atomistic modeling of laser-related phenomena. InLaser Annealing Processes in Semiconductor Technology 2021 Jan 1 (pp. 79-136). Woodhead Publishing.*
17. *Dreuw A, Wormit M. The algebraic diagrammatic construction scheme for the polarization propagator for the calculation of excited states. Wiley Interdisciplinary Reviews: Computational Molecular Science. 2015 Jan;5(1):82-95.*

18. *Urquhart RJ, Tuttle T. Computational modeling of 4d and 5d transition metal catalysts. InReference Module in Chemistry, Molecular Sciences and Chemical Engineering 2023 Feb 23.*

19. *Christensen AS, Kubar T, Cui Q, Elstner M. Semiempirical quantum mechanical methods for noncovalent interactions for chemical and biochemical applications. Chemical Reviews. 2016 May 11;116(9):5301-37.*

20. *Goh GB, Hodas NO, Vishnu A. Deep learning for computational chemistry. Journal of computational chemistry. 2017 Jun 15;38(16):1291-307.*

21. *. Burke K, Wagner LO. DFT in a nutshell. International Journal of Quantum Chemistry. 2013 Jan 15;113(2):96-101*

22. *. Hollebon P, Sjostrom T. Hybrid Kohn-Sham+ Thomas-Fermi scheme for high-temperature density functional theory. Physical Review B. 2022 Jun 13;105(23):235114.*

23. *Helgaker T, Coriani S, Jørgensen P, Kristensen K, Olsen J, Ruud K. Recent advances in wave function-based methods of molecular-property calculations. Chemical reviews. 2012 Jan 11;112(1):543-631.*

24. *Assadi MH, Hanaor DA. Theoretical study on copper's energetics and magnetism in TiO2 polymorphs. Journal of Applied Physics. 2013 Jun 21;113(23).*

25. *Chandrasekaran B, Abed SN, Al-Attraqchi O, Kuche K, Tekade RK. Computer-aided prediction of pharmacokinetic (ADMET) properties. InDosage form design parameters 2018 Jan 1 (pp. 731-755). Academic Press.*

26. *. Bajorath J. Selected concepts and investigations in compound classification, molecular descriptor analysis, and virtual screening. Journal of chemical information and computer sciences. 2001 Mar 26;41(2):233-45.*

27. *. Jensen F. Introduction to computational chemistry. John wiley & sons; 2017 Feb 6.*

28. *Guan L, Yang H, Cai Y, Sun L, Di P, Li W, Liu G, Tang Y. ADMET-score–a comprehensive scoring function for evaluation of chemical drug-likeness. Medchemcomm. 2019;10(1):148-57.*

29. *van Lonkhuizen PJ, Klaver KM, Wefel JS, Sitskoorn MM, Schagen SB, Gehring K. Interventions for cognitive problems in adults with brain cancer: a narrative review. European journal of cancer care. 2019 May;28(3):e13088.*

30. *Nguyen L, Van Hoeck A, Cuppen E. Machine learning-based tissue of origin classification for cancer of unknown primary diagnostics using genome-wide mutation features. Nature communications. 2022 Jul 11;13(1):4013.*

31. *Balasubramani G, Muthu M, Gopal J, Chun S. A review on the impact of TRAIL on cancer signaling and targeting via phytochemicals for possible cancer therapy. International Journal of Biological Macromolecules. 2023 Oct 1:127162.*

32. *Ali I, Hozaifa M, Ali S, Malik A, Locatelli M. Advances in ionic liquids as future anti-cancer drugs. Journal of Molecular Liquids. 2023 Aug 12:122823.*

33. *Zhang Z, Yang Y, Xu Y, Liu Y, Li H, Chen L. Molecular targets and mechanisms of anti-cancer effects of withanolides. Chemico-Biological Interactions. 2023 Sep 9:110698.*

34. *Kowe PA, Madke B, Bansod SH. Oral minoxidil in trichology: A review. Indian Journal of Drugs in Dermatology. 2022 Jan 1;8(1):1.*

35. *Kowe PA, Madke B, Bansod SH. Oral minoxidil in trichology: A review. Indian Journal of Drugs in Dermatology. 2022 Jan 1;8(1):1.*

36. *Laurent S. Antihypertensive drugs. Pharmacological research. 2017 Oct 1;124:116-25.*

37. *Metwally NH, Mohamed MS, Ragb EA. Design, synthesis, anticancer evaluation, molecular docking and cell cycle analysis of 3-methyl-4, 7-dihydropyrazolo [1, 5-a] pyrimidine derivatives as potent histone lysine demethylases (KDM) inhibitors and apoptosis inducers. Bioorganic Chemistry. 2019 Jul 1;88:102929.*

38. *Muthuraja P, Veeramani V, Prakash S, Himesh M, Venkatasubramanian U, Manisankar P. Structure-activity relationship of pyrazolo pyrimidine derivatives as inhibitors of mitotic kinesin Eg5 and anticancer agents. Bioorganic Chemistry. 2019 Mar 1;84:493-504.*

39. *Nasser AA, Eissa IH, Oun MR, El-Zahabi MA, Taghour MS, Belal A, Saleh AM, Mehany AB, Luesch H, Mostafa AE, Afifi WM. Discovery of new pyrimidine-5-carbonitrile derivatives as anticancer agents targeting EGFR WT and EGFR T790M. Organic & biomolecular chemistry. 2020;18(38):7608-34.*

40. *Wang R, Yu S, Zhao X, Chen Y, Yang B, Wu T, Hao C, Zhao D, Cheng M. Design, synthesis, biological evaluation and molecular docking study of novel thieno [3, 2-d] pyrimidine derivatives as potent FAK inhibitors. European Journal of Medicinal Chemistry. 2020 Feb 15;188:112024*

41. *Bommera RK, Kethireddy S, Govindapur RR, Eppakayala L. Synthesis, biological evaluation and docking studies of 1, 2, 4-oxadiazole linked 5-fluorouracil derivatives as anticancer agents. BMC chemistry. 2021 Dec;15:1-2*

42. *Mumit MA, Pal TK, Alam MA, Islam MA, Paul S, Sheikh MC. DFT studies on vibrational and electronic spectra, HOMO–LUMO, MEP, HOMA, NBO and molecular docking analysis of benzyl-3-N-(2, 4, 5-trimethoxyphenylmethylene) hydrazinecarbodithioate. Journal of molecular structure. 2020 Nov 15;1220:128715.*

43. *Berthel SJ, Cheung AW, Kim K, Li S, Thakkar KC, Yun W, inventors. Pyridopyrimidine protein tyrosine phosphatase inhibitors. United States patent application US 12/837,558. 2010 Nov 4.*

44. *Tiwari A, Singh S. Computational approaches in drug designing. InBioinformatics 2022 Jan 1 (pp. 207-217). Academic Press*.

45. *Bochevarov AD, Harder E, Hughes TF, Greenwood JR, Braden DA, Philipp DM, Rinaldo D, Halls MD, Zhang J, Friesner RA. Jaguar: A high-performance quantum chemistry software program with strengths in life and materials sciences. International Journal of Quantum Chemistry. 2013 Sep 15;113(18):2110-42.*

46. *Carey FA, Sundberg RJ. Advanced organic chemistry: part A: structure and mechanisms. Springer Science & Business Media; 2007 Jun 13.*

47. *Tallei TE, Tumilaar SG, Niode NJ, Kepel BJ, Idroes R, Effendi Y, Sakib SA, Emran TB. Potential of plant bioactive compounds as SARS-CoV-2 main protease (M pro) and spike (S) glycoprotein inhibitors: a molecular docking study. Scientifica. 2020 Dec 23;2020.*

48. *Sun J, Wen M, Wang H, Ruan Y, Yang Q, Kang X, Zhang H, Zhang Z, Lu H. Prediction of drug-likeness using graph convolutional attention network. Bioinformatics. 2022 Dec 1;38(23):5262-9.*

49. *Mkhayar K, Haloui R, Daoui O, Elkhattabi K, Chtita S, Elkhattabi S. In silico studies of 2-aryloxy-1, 4-naphthoquinone derivatives as antibacterial agents against Escherichia coli using 3D-QSAR, ADMET properties, molecular docking, and molecular dynamics. Chemical Data Collections. 2023 Oct 1;47:101060.*

50. *Ivanović V, Rančić M, Arsić B, Pavlović A. Lipinski's rule of five, famous extensions and famous exceptions. Popular Scientific Article. 2020;3(1):171-7.*

51. *Chandrasekaran B, Abed SN, Al-Attraqchi O, Kuche K, Tekade RK. Computer-aided prediction of pharmacokinetic (ADMET) properties. InDosage form design parameters 2018 Jan 1 (pp. 731-755). Academic Press.*

52. *Chen X, Li H, Tian L, Li Q, Luo J, Zhang Y. Analysis of the physicochemical properties of acaricides based on Lipinski's rule of five. Journal of computational biology. 2020 Sep 1;27(9):1397-406.*

53. *Hajji H, Alaqarbeh M, Lakhlifi T, Ajana MA, Alsakhen N, Bouachrine M. Computational approach investigation bioactive molecules from Saussurea Costus plant as SARS-CoV-2 main protease inhibitors using reverse docking, molecular dynamics simulation, and pharmacokinetic ADMET parameters. Computers in Biology and Medicine. 2022 Nov 1;150:106209.*

54. *Wei M, Zhang X, Pan X, Wang B, Ji C, Qi Y, Zhang JZ. HobPre: accurate prediction of human oral bioavailability for small molecules. Journal of Cheminformatics. 2022 Dec;14(1):1-0.*

55. *Davis JL. Pharmacologic principles. Equine internal medicine. 2018;4:79-137*

56. *Wang Y, Xing J, Xu Y, Zhou N, Peng J, Xiong Z, Liu X, Luo X, Luo C, Chen K, Zheng M. In silico ADME/T modelling for rational drug design. Quarterly reviews of biophysics. 2015 Nov;48(4):488-515.*

57. *Setyawati LU, Parlan FI, Ikram NK, Yusuf M, Muchtaridi M. Molecular Dynamic Simulation and 3d-pharmacophore Modeling of Alpha Mangostin and Its Derivatives Against Estrogen Alpha Receptor.*